Functionalised Adsorbents for Removal and Recovery of Precious Metals and Chromium from Aqueous Solutions

Marta O.N.A. Elvin[1,2*], Mathew M. Nindi[1], Habauka M. Kwaambwa[2] and Simi Dube[1]

[1]*Department of Chemistry, College of Science Engineering and Technology, University of South Africa, Johannesburg, South Africa.*
[2]*Faculty of Health, Natural Resources and Applied Sciences, Namibia University of Science and Technology, Windhoek, Namibia.*

ABSTRACT

Precious metals (PMs) such as palladium (Pd), platinum (Pt), and gold (Au) are economically valuable elements that commonly co-exist with toxic chromium(VI) [Cr(VI)] in industrial effluents. However, effective techniques for recovering or removing them from these wastewater streams remain a technological and critical environmental challenge. There is a limited comparative evaluation of various studies on functionalised adsorbents that have proven capability for wastewater treatment. Systematic and consolidated evaluation of functionalised adsorbents for the recovery or removal of PMs and Cr(VI) is offered in this review. Current developments in production and functionalisation approaches, characterisation techniques, adsorption studies (models, equilibrium, mechanisms), recovery and recycling methods are distinctly integrated. The reasonable framework informing the realistic layout and optimisation of future adsorbents by carefully investigating performance trends and identifying predominant gaps is demonstrated in the review. The perceptions reported are meant to support the enhancement of sustainable, effective, and scalable techniques applicable to wastewater remediation in mining, industrial, and emergingeconomy settings.

KEYWORDS

adsorption, functionalised adsorbent, heavy metal ion, precious metals, wastewater

Received: 21 November 2025 Revised: 22 April 2026 Accepted: 23 May 2026

INTRODUCTION

PMs, namely palladium, gold, and platinum, are widely used in jewellery, catalysis, and electronics due to their outstanding resistance to oxidation and conductivity.[1,2] They extensively accumulate in electronic waste streams and industrial effluents because of their cumulative usage in modern technologies.[3] These metals are mostly found in endoflife electrical components, mainly printed circuit boards, resulting in secondary waste mining being an attractive approach for circulareconomy development, resource recovery, and preservation of deteriorating primary mineral investments.[4] Despite their economic value, PMs, if released uncontrollably into marine systems, raise ecological concerns, necessitating efficient removal and recovery techniques.

Hexavalent chromium [Cr(VI)], commonly coexits with PMs in effluent water released from tanning, mining, and other similar industries.[3-5] It is against this background that integrated treatment techniques are required for both PMs and Cr(VI). Research has demonstrated that functionalised adsorbents present an exceptionally adaptable platform as they are capable of being engineered for great selectivity of recovery of PMs while at the same time offering electrostatic pathways or redoxactive sites for Cr(VI) removal. This two-fold functionality features their applicability for complex effluent treatment systems capable of addressing contamination from both PMs and Cr(VI).

Compared to trivalent chromium [Cr(III)], which is biologically important and relatively benign in lower concentrations, Cr(VI) is exceedingly poisonous and oncogenic to species that are both persistent and mobile in aqueous environments, which is a major regulatory concern. Effluent contaminated with Cr(VI) also contains trace amounts of other heavy metals, namely mercury, arsenic, iron, cadmium, copper, and nickel.[5]

These heavy metals remain chemically stable under extreme ecological conditions, are bioaccumulative and nonbiodegradable, which is different from most organic pollutants, thus posing other challenges. Due to these, it is a challenge to treat them successfully with conventional techniques. The emphasis by international guidelines, mainly the World Health Organization, is to maintain extremely low levels of chromium in drinking water at (<0.05 mg/L) due to the associated carcinogenic, hepatic, and renal health impacts.[5]

Various techniques have been employed to recover or remove PMs and Cr(VI), namely membrane filtration, ion exchange, chemical precipitation, cementation, solventbased, and flotation methods.[6–8] Even though they are extensively used, these conventional approaches often suffer reduced effectiveness, high operational costs, and inadequate selectivity when handling largevolumes or dilute wastes.[5] As a result, adsorption has been demonstrated to be an attractive option because of its compatibility, costeffectiveness, simplicity, and scalability.[9–11]. Activated carbon (AC), biomaterials, metal oxides, polymers, clay minerals, graphenebased, and silica materials are among several adsorbents that have exhibited favorable performance in treating effluent contaminated with metal ions.[5,8,12] Nonetheless, these materials also present remarkable weaknesses. For instance, AC commercially produced from conventional precursors (e.g., charcoal, coconut shells, and wood) is expensive, stimulating interest in inexpensive industrial and agricultural options for carbon sources.[13,14] Equally, graphenebased clays and unmodified silica adsorbents regularly demonstrate surface heterogeneity, inadequate affinity, and restricted selectivity for definite metal species, particularly under complex wastewater environments. Due to these limitations, functionalisation approaches that adapt adsorbent surfaces with hybrid structures or specific chemical groups are essential. Functionalisation improves stability and dispersion, selectivity, increases binding affinity, and allows adsorbents to target numerous metal ions, including Cr(VI) and PMs, inside mixedcontaminant systems. Subsequently, functionalised adsorbents represent a further effective and useful pathway for complex effluent treatment and resource recovery.

Carbonbased nanomaterials (CNMs) have been attractive due to their favourable reactivity, tunable chemistry, and large surface area.[5,15] Conversely, their adsorption effectiveness is frequently reduced by their tendency to aggregate in aqueous systems. CNMs functionalisation using noncovalent or covalent attachment of specific

*To whom correspondence should be addressed
Email: 21078009@mylife.unisa.ac.za/melvin@nust.na

ISSN 1996-840X Online / South African Chemical Institute / http://saci.co.za/journal
© The Author(s) Published under a Creative Commons Attribution 4.0 International Licence (CC BY 4.0)
https://doi.org/10.17159/0379-4350/2026/v80se1a17

groups has become a popular approach to enhance stability, dispersion, and attraction toward metal ions. Of these, functionalisation using non-covalent attachment is mostly fascinating because it improves biocompatibility and solubility without interrupting the πconjugated assembly of the carbon matrix. Functionalised CNMs combined with polymers and metal oxides to form hybrid nanocomposites display synergistically improved characteristics, such as enhanced electrical and mechanical properties, wider surface area, and increased selectivity for metal ion binding. Approaches such as chemical vapour processes, hydrothermal techniques, templateassisted routes, and sol–gel processing can be used to produce these materials.

Magnetic iron oxides such as γFe_2O_3, αFe_2O_3, and Fe_3O_4 are often integrated to aid in easy magnetic separation and recycling[16] whereas natural products, namely zeolites, surfactants, and Moringa extracts, can further enhance adsorption capacity.[17] Functionalisation of adsorbents for treatment of effluent contaminated with metal ions, such as PMs and Cr(VI) adsorbents has made substantial advancement. Nonetheless, prevailing studies are distributed across numerous research domains, repeatedly concentrating on isolated aspects such as specific characterisation or synthesis techniques, the remediation of a single metal ion, and the performance of individual adsorbents. Comparative and integrated analysis connecting adsorption mechanisms, structural characteristics, and functionalisation strategies for both PMs and Cr(VI) is lacking in the literature. In addition, broad assessment of adsorption models, equilibrium, mechanism, kinetics, recovery, and reusability competencies is also limited, although fundamental for evaluating realistic applicability.

Essential and efficient assessment of functionalised adsorbents for the recovery and removal of PMs and Cr(VI) from aqueous systems is provided by this review to address these gaps. It focuses on materials synthesis and functionalisation, applying established physicochemical models to assess adsorption performance, and explores reuse and regeneration approaches. The aim is to determine a consistent framework that supports the rational optimisation and design of future adsorbents appropriate to industrial effluent remediation and recovery of resources.

ADSORBENT SUBSTRATES SYNTHESIS APPROACHES AND THEIR FUNCTIONALISATION

To improve selectivity, stability, and performance of adsorbents applied in the recovery of PMs and removal of Cr(VI), an extensive range of synthesis and functionalisation methods has been developed. Three main functionalisation categories, namely hybrid or composite functionalization, surfacechemical functionalization, and biofunctionalisation, have been identified so that these approaches are not viewed as isolated systems. This structure enables direct comparison of their efficiency, stability, and applicability across different wastewater matrices.

Surface chemical functionalisation

Chemical functionalisation techniques such as chemical vapour deposition (CVD), sol–gel synthesis, hydrothermal treatment, and acid/base modification are widely used to introduce functional groups including amines ($-NH_2$), carboxyls (–COOH), and thiols (–SH). These groups improve adsorbent affinity toward PMs through coordination bonding and enhance Cr(VI) reduction by providing redox-active or proton-donating sites.

The effectiveness of these approaches has been demonstrated in several studies. For example, Egbosiuba et al.[18] produced an MWCNTs–KIAgNPs composite using chemical vapour deposition (CVD and green-synthesised silver nanoparticles from *Khaya ivorensis* leaves, incorporating hydroxyl and carboxyl groups to enhance physicochemical properties. Oxidative functionalisation of carbon nanomaterials introduces negatively charged oxygen-containing groups, increasing dispersion and generating strong binding sites for metal ions. Similarly, silver-decorated MWCNT composites combine oxidative surface groups with metal nanoparticle catalytic sites, improving both PM uptake and Cr(VI) reduction.

In another example, Padmavathy et al.[19] applied the sol–gel method to synthesize magnetite nanoparticles, which exhibited uniform particle size and abundant surface hydroxyl groups, resulting in improved Cr(VI) reduction capabilities.

Despite these advantages, chemical functionalisation techniques can present challenges such as acidic corrosion of carbon frameworks, aggregation of metal oxide particles, and loss of functional groups during repeated regeneration, which may compromise long-term stability in real wastewater systems.

Biofunctionalisation

Bio-functionalisation involves the use of biopolymers or biomolecules (e.g., proteins, polysaccharides, plant extracts) to introduce naturally occurring functional groups such as amines, amides, hydroxyls, and carboxylates onto metal oxide or carbon surfaces. These biomolecules provide dense and multifunctional binding sites that enhance selectivity toward PMs while also supporting the redox interactions required for Cr(VI) reduction. In one example, Amuanyena et al.[20] employed *Moringa oleifera* seed protein extract to modify Fe_3O_4 nanoparticles synthesized from iron salts, with the seed proteins prepared following the method of Maikokera and Kwaambwa.[21] The resulting bio-functionalised nanoparticles formed aminerich surface layers that improved selectivity toward Au(III), Pd(II), and Pt(IV), while also increasing negative surface charge at elevated pH, a property that may further promote Cr(VI) removal. Although bio-functionalisation offers advantages such as biodegradability, mild synthesis conditions, and low toxicity, these systems may still face limitations, including thermal instability, susceptibility to biodegradation, and sensitivity to pH or ionic strength during repeated adsorption-desorption cycles.

Hybrid and composite functionalisation

Hybridisation strategies integrate polymers, metal oxides, layered double hydroxides (LDHs), and carbonaceous materials into a single nanocomposite, enabling systems that combine magnetic separability, high surface area, tunable surface chemistry, and mechanical stability. In one example, Biata et al.[22] synthesised a magnetic iron oxide/MgAlLDH nanocomposite using a coprecipitation method, which exhibited high anionexchange capacity for Cr(VI) and strong electrostatic attraction toward PM–chloride complexes. Findings from this study highlight that hybrid materials often deliver superior adsorption capacities, improved regeneration stability, and efficient magnetic recoverability. However, these advantages may be offset by the need for multistep synthesis procedures, higher production costs, and potential drawbacks such as nanoparticle leaching or reduced performance in highsalinity wastewater.

Chemical vapour deposition, template-assisted synthesis, hydrothermal and sol–gel methods are commonly used methods to produce functionalised adsorbents. Surfaces of these adsorbents are functionalised to enhance adsorption by introducing several functional groups, such as amine ($-NH_2$), carboxyl (–COOH), and thiol (–SH). The performance of nanomaterials could be boosted further through hybridisation (integration) with polymers and metal oxides, resulting in the production of nanocomposites with enhanced properties.

Activated carbon (AC) is a popular adsorbent applied nowadays, which is prepared using two fundamental phases: carbonisation and activation.[18–20] Volatile substances are removed through the carbonisation process, which involves heating at temperatures between 425–525 °C in an inert atmosphere (without oxygen and usually with nitrogen or argon). Chemical, physical, or a combination of the two can be used for the activation process. Physical activation involves heating at temperatures between (825–1 025 °C) and in the presence of air for the surface to be porous and widen. For chemical activation, the

initial material is treated with chemical agents before carbonisation, and this is usually done at lower temperatures and results in a highly porous carbon structure. Decomposition of organic materials is carried out in the absence of oxygen between 400-700 ˚C, producing biochar. Carbon for activation is produced by the carbonisation method, removing volatile substances, hence enriching the carbon content and creating a suitable substrate for the activation process. The physicochemical properties, including porosity and surface area of the AC, are enhanced by the activation stage. When using lignin-based materials as a precursor, the activation process involves treating the carbonised material with activation chemicals, which help to inhibit the formation of tars and create a porous structure with few holes on the surface. The existing holes are mainly widened by burning the walls dividing them. Physical activation mainly uses carbon dioxide (CO_2). In contrast, zinc chloride, potassium hydroxide, phosphoric acid and sodium hydroxide are drying agents applied in chemical activation. However, compared to chemical activation, physical activation tends to produce AC with a lower value and yield due to extended activation time and extreme temperature.

Biata et al.[21] applied a co-precipitation approach to synthesise a magnetic iron oxide/MgAl-LDH nanocomposite. Briefly, a sonicator was used to mix 100 mL of solution containing a 1:1 methanol: water ratio and iron oxide. The mixing time was about 15 minutes. Sodium hydroxide (NaOH) and sodium carbonate in a water: methanol (1:1) ratio created solution (A). Solution (A) was mixed dropwise with a methanol/water mixture (100mL) containing the Fe_3O_4 nanoparticles till pH of 10 was obtained, then left to settle for five minutes. To make up solution (B), $AlCl_3$ and $MgCl_2.6H_2O$ were mixed in a water: methanol ratio (1:1), then allowed to age for 24 h at 60 ˚C. The product was collected using a magnet, washed with distilled water, and allowed to dry for 12 h at 60 ˚C.

Using a procedure by Maikokera and Kwaambwa,[22] as cited in Amuanyena et al.,[23] seed proteins from *Moringa oleifera* were prepared: Petroleum ether was used to remove oil from *M. oleifera* seed powder. The defatted powder was transferred to a 1 M potassium chloride solution. A clear solution was obtained by first suction filtration and lastly gravity. Ammonium sulphate was used to extract the proteins by forming a sticky paste through the "salting out" effect. Suction filtration was used for filtration. The paste was again dissolved in water, and a dialysis tube made from cellulose was used for dialysis. A solution of sodium chloride (1M) was used to recover the protein after the CMC resin was used for purification, then dialysed again, and thereafter freeze-dried. Amuanyena et al.[23] used *Moringa oleifera* seed protein extract to modify Fe_3O_4 nanoparticles prepared from iron salts using the following procedure: A 1% 20mL Moringa protein solution containing iron(III) chloride and iron(II) chloride (2:1) was prepared and properly mixed for 20 min. In a different container, another Moringa protein solution (1%) was used to prepare a sodium hydroxide (8 M) solution, which was prepared under ice and mixed at 25 °C for 30 min. Fe_3O_4 modified with *M. oleifera* seed proteins was precipitated by continuously mixing the two solutions for 1 h. The magnet was used to collect the black nanoparticles. Acetone and water were used to remove impurities from the nanoparticles; thereafter, the product was freeze-dried and kept in an airtight container until ready for use.

Padmavathy et al.[24] used the sol–gel method to produce magnetite nanoparticles for the remediation of wastewater containing Cr(VI). 0.020 mol of $Fe(NO_3)3{\cdot}9H_2O$ and 25 mL of $(CH_2OH)_2$ were mixed with a magnetic stirrer at 20 °C for 3 h. The mixture was continuously stirred and allowed to reach 80 °C. The obtained product was cooled to 20 °C for 1 h and dried in an oven. An annealing process was carried out at 400 °C to obtain black nanoparticles.

Egbosiuba et al.[25] used green chemistry and chemical vapour deposition processes to produce an MWCNTs-KIAgNPs composite by using silver nanoparticles (AgNPs) synthesised via green chemistry using *Khaya ivorensis* leaves (KIAgNPs) and multi-walled carbon nanotubes (MWCNTs). To incorporate the functional groups, namely, hydroxyl and carboxyl to enhance the physicochemical properties of the composite, two stages were followed in the preparation. The initial phase involves a combination of H_2SO_4 and HNO_3 in a ratio of 3:1 with MWCNTs to allow for the incorporation of negatively charged functional groups. Mixing was done using an ultrasonic bath at 40 °C for 3 h to ensure that the functional groups are incorporated. After filtering, distilled water was used to wash until a pH of 7. Functionalised MWCNTs were dried in an oven overnight at 110 °C. During phase two, the properties of the functionalised MWCNTs were improved using KIAgNPs. In this phase, sonication for 3 h was used to allow MWCNTs and KIAgNPs attach in dimethylformamide (DMF). The obtained composite was then cleaned and dried using the same procedure as that used for the functionalised MWCNTs. The product was kept in an airtight vial until use.

CHARACTERISATION TECHNIQUES

The physicochemical characteristics of the nanomaterials are assessed using various characterisation methods. These include vibrating sample magnetometry (VSM), X-ray diffraction (XRD), scanning electron microscopy (SEM), zeta potential analysis (ZPA), thermogravimetric analysis (TGA), Brunauer-Emmett-Teller (BET) method, and Fourier transform infrared spectroscopy (FTIR).

X-ray diffraction

Xray diffraction (XRD) is a primary technique used for crystal structure confirmation of the successful functionalisation phase composition of adsorbents developed for precious metal (PM) recovery and Cr(VI) remediation. Beyond simple phase identification, XRD is particularly valuable for demonstrating that surface modification or composite formation has occurred without compromising the crystalline features responsible for adsorption, redox activity, and magnetic recovery.

XRD allows identification of semicrystalline and crystalline phases via representative diffraction patterns evolving from longrange atomic order, as highlighted by Mourdikoudis et al.[23] Although carbonaceous matrices repeatedly display amorphous features that are broad, strong evidence of successful integration of metallic or inorganic phases after functionalisation is provided when sharp reflections appear. It is essential to preserve these diffraction structures after, as crystallographic sequence directs electron transfer pathways, mechanical stability, and magnetic response during repetitive adsorption–desorption cycles.

Anyika et al.,[16] used powder XRD to confirm the synthesis of magnetic activated carbon (MGAC), which further provided a clear illustration of the validation role of this technique. Diffuse, broad reflections characterising predominant amorphous carbon were displayed by the raw carbon precursors. Conversely, intense, sharp diffraction peaks related to iron oxide phases scanned at 2θ (20–100°) were displayed by functionalised MGAC. The presence of magnetite (Fe_3O_4), which is a primary phase liable for magnetic separability, was confirmed when comparisons were made with JCPDS reference standards [24]. To verify that ironbased functional groups were successfully impregnated into the porous carbon matrix, rather than being physically mixed or loosely associated, these crystalline iron oxide reflections emerged within the amorphous carbon background. The recovery of PMs and removal of Cr(VI) critically require this structural confirmation, where redoxactive iron sites and magnetic responsiveness facilitate efficient adsorption, posttreatment separation, and reduction.

Nanoscale crystallinity in carbonbased nanocomposites is further confirmed using XRD. For instancee, diffraction peaks at 2θ = 26.55°, 38.32°, 44.50°, 64.59°, 74.65°, 77.55°, and 81.80° for MWCNTsKIAgNPs were reported by Egbosiuba et al.[18] These peaks correspond to the carbon framework and integrated silver nanoparticles. Using the Debye–Scherrer equation, the crystallite size of 11.30 nm was obtained, which confirms nanoscale domains that improve adsorption capacity and surface accessibility for Cr(VI) and PMs. These peaks are

retained after functionalisation, which indicates that the underlying carbon lattice is not interrupted by nanoparticle decoration, which support steady adsorption performance.

Direct evidence of PMs recovery mechanisms in chemically activated carbons is also provided by XRD. Celluloserelated reflections at 15.9° and 21.6°, together with broader graphitelike reflections between 27° and 44° after activation, were obtained by Bediako et al.,[25] using sulphuricacidactivated carbon synthesised from orange peel biomass. A reduction of Au(III) to a facecentred cubic metallic gold Au(0) was confirmed by new reflections at 37.9°, 44.2°, 64.4°, and 77.6°, indexed at (311), (220), (200), and (111) after adsorption. This demonstrates the adsorbent functions as a reactive recovery platform, not a passive adsorbent.

XRD confirms iron oxide crystallite size and phase identity, which directly influence reduction and adsorption efficiency for the removal of Cr(VI).[26] Magnetite (Fe_3O_4) nanoparticles with a crystallite size of 56 nm were obtained by Padmavathy et al.,[19] whereas smaller crystallites of 22.325 nm were reported by Mittal et al.[27] having reflections at 24.1° and 35.6°, suggesting increased exposure of Fe sites, which are redoxactive. Generally, XRD creates robust structure–function interactions, confirming functionalisation approaches and validating the appropriateness of adsorbents for Cr(VI) removal and PMs.

Zeta potential analysis

This technique is extensively applied to assess both the success of surface functionalisation and the colloidal stability of nanomaterials because it clearly exhibits deviations in surface charge developing from chemical modification.[23] In functionalised adsorbents, a measurable shift in ζpotential magnitude or in the isoelectric point (IEP) relative to the unmodified material provides evidence that new functional groups have been successfully introduced onto the surface. Zeta potential represents the electrokinetic potential at the slipping plane of a particle in suspension and is a key indicator of dispersion stability.

Mourdikoudis et al.[23] reported that particles with ζpotential values above +30 mV or below −30 mV exhibit strong electrostatic repulsion and are therefore resistant to aggregation, while values closer to zero promote agglomeration. Since functionalisation alters surface chemistry, it changes the surface charge distribution and, consequently, the ζpotential and stability of the material. Kumar and Dixit,[28] similarly described ζpotential as a measure of the net surface charge arising from functional groups and counterion layers at the particle–solution interface, making it particularly useful for evaluating surface modification.

The application of ζpotential analysis to confirm functionalisation is illustrated by Amuanyena et al.,[20] (Figure 1) who studied Fe_3O_4 nanoparticles modified with Moringa oleifera seed protein extract. The modified nanoparticles exhibited a lower isoelectric point (pH 3.69) compared to unmodified Fe_3O_4 (pH 6.12), confirming the successful attachment of protein functional groups to the surface. The altered ζpotential behaviour across the pH range further explains the pHdependent adsorption of precious metal ions, as surface charge governs electrostatic interactions with metal species in solution. Optimal adsorption from pH 4.0 and 6.0 was observed by Shekede and Mishra,[29] and reported similar trends that are pHdependent.

The role of ζpotential analysis in nanocomposites was further demonstrated by Biata et al.,[27] for the recovery of Au(III) and Ir(IV). A positively charged adsorbent surface over a wide pH range was confirmed with an isoelectric point value of 10.5, which explains the strong electrostatic attraction toward negatively charged PM complexes and confirms a successful functionalisation. Conversely, a ζpotential value of −31.5 mV was reported by Mittal et al.[28] using Spirulinaderived mesoporous Fe_3O_4 nanoparticles in the remediation of Cr(VI) confirms both effective surface functionalisation by biomolecules from the algal extract and good colloidal stability.

Generally, successful functionalisation is significantly confirmed through ζpotential analysis by enhanced dispersion stability, revealing changes in surface charge and isoelectric point. These measurements present a systematic perception into how surface modification improves Cr(VI) and PMs removal and recovery when combined with adsorption data.

Scanning electron microscopy

This technique is used to assess porosity, texture, particle size, and surface morphology, which are strongly enhanced by surface functionalisation.[23] A scanning electron microscope (SEM) is often coupled with energydispersive Xray spectroscopy (EDX) to provide spatial mapping and elemental composition, which enables researchers to verify the distribution and presence of adsorbed species or heteroatoms introduced during adsorption or modification.[30] Based on this, the technique is essential since it is not just a descriptive tool but also useful for adsorption performance and for validating successful functionalisation.

Images provided by SEM facilitate explicit visualisation of structural modifications developing from surface modification, such as altered particle aggregation, pore development, and increased roughness. SEM micrographs evidently differentiate between inorganic and

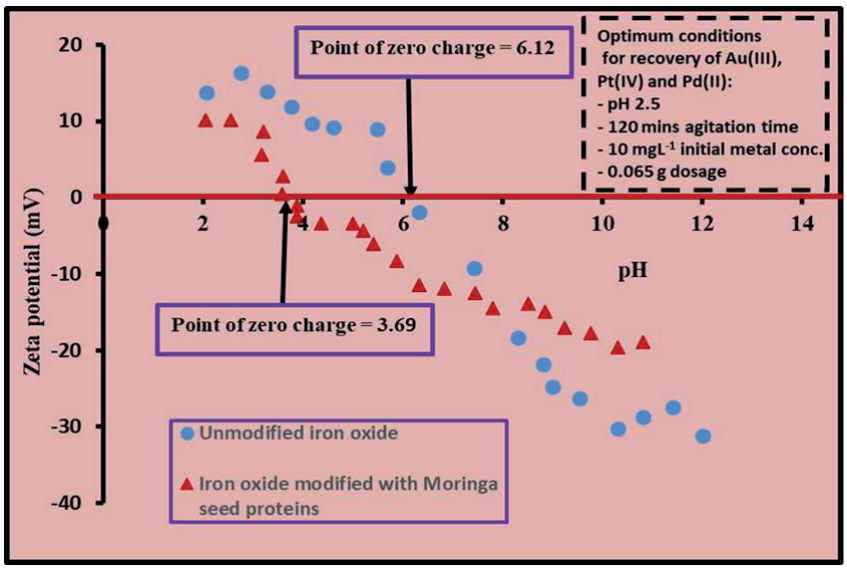


Figure 1. Zeta potential trends for unmodified and modified Fe_3O_4 nanoparticles with *M. oleifera* seed protein extract (reproduced from Amuanyena et al. 2019[20] with permission).

organic materials, as demonstrated by Anyika et al.[16] This study further emphasised that SEM and Transmission electron microscope (TEM) are crucial for linking structural features with physicochemical characteristics. Functionalisation regularly leads to visible modifications in porosity and surface texture, which can be directly correlated to improved accessibility of active adsorption sites and surface area.

SEM images (Figure 2) showing a more heterogeneous surface and improved porosity features of Fe_3O_4 nanoparticles modified with Moringa oleifera seed protein in comparison to unmodified Fe_3O_4 were illustrated by Amuanyena et al.[20] The successful surface modification is confirmed by these morphological changes and clarifies the improved adsorption performance, as surface irregularities and enhanced pore density offer further available binding sites for PMs.

Functionalisation evidence is further strengthened by SEM–EDX analysis, verifying elemental changes linked to surface adsorption or modification. The SEM–EDX was used by Zhu, Zhu, and Huang[30] to characterise a biosorbent derived from modified pomegranate peel. A transformation from a soft, fluffy surface before adsorption to a more compact structure with adhered particles post adsorption was revealed using SEM images, whereas the presence of precious metals, oxygen, and chlorine on the surface was confirmed with EDX mapping. The appearance of these elements confirms both the successful binding of PMs and the introduction of functional groups.

SEM–EDX images of Fe_3O_4 nanoparticles displayed regular oxygen and iron distributions, demonstrating uniform surface composition in a study by Padmavathy et al.[19] to remove Cr(VI). Successful modification was further confirmed by Ihsanullah et al.[31] when acid treatment of carbon nanotubes changed the AC surface texture and reduced CNT lengths. These structural modifications were clearly linked to increased surface area and pore volume, which in turn improved adsorption capacity.

Generally, analyses using SEM–EDX and SEM are vital for verifying successful functionalisation by revealing porosity changes and morphology introduced by surface modification, verifying elemental adsorption or integration, and associating structural evolution to enhanced adsorption efficiency.

Thermogravimetric analysis

Thermogravimetric analysis (TGA) is a powerful characterisation technique for evaluating the thermal stability, composition, and degree of surface functionalisation of adsorbent materials by monitoring mass changes as a function of temperature under controlled atmospheres.[23] In functionalised materials, TGA is particularly useful for confirming the presence, thermal behaviour, and relative quantity of surfacebound functional groups, as these groups decompose or volatilise at characteristic temperature ranges distinct from the inorganic support.

TGA measurements are performed by heating a known mass of material under inert or oxidative conditions while continuously recording weight changes with microgram precision.[16,32] Weight losses observed at low temperatures are typically associated with physisorbed or bound water, whereas additional mass losses at higher temperatures indicate the decomposition of organic functional groups or surface modifiers. By comparing TGA profiles of modified and unmodified materials, successful functionalisation can therefore be confirmed through the appearance of new decomposition steps, shifts in thermal events, or changes in overall mass loss. This approach is illustrated by Amuanyena et al.[20] (Figure 3-4) who compared unmodified Fe_3O_4 nanoparticles with Fe_3O_4 functionalised using Moringa seed protein extract. The multistep weightloss behaviour observed for the modified material, particularly in the 100–350 °C range, was attributed to the thermal decomposition of proteinbased organic functional groups. The presence of these additional massloss stages, not prominent in the unmodified Fe_3O_4, confirmed successful surface modification. Variations in overall weight loss between unmodified and modified materials further provided insight into the thermal stability and the amount of the attached functional groups.

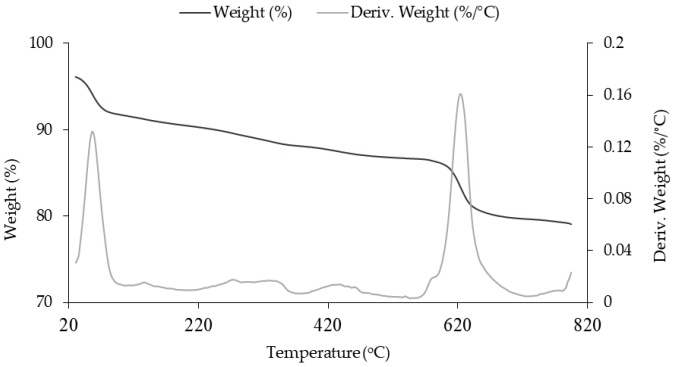


Figure 3. TGA curve for unmodified Fe_3O_4 nanoparticles (reproduced from Amuanyena et al. 2019 [20] with permission).

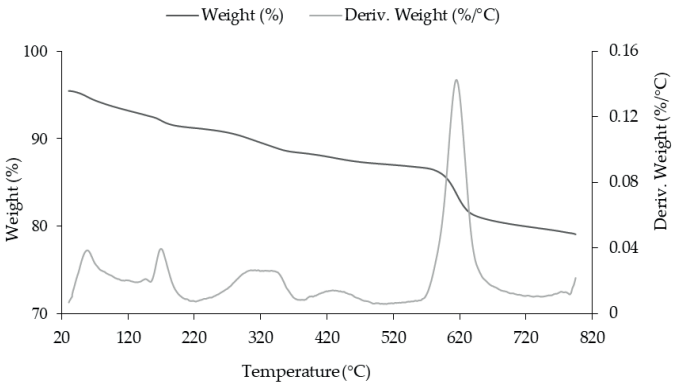


Figure 4. TGA curve for Fe_3O_4 nanoparticles modified with *M. oleifera* seed protein (reproduced from Amuanyena et al. 2019 [20] with permission).

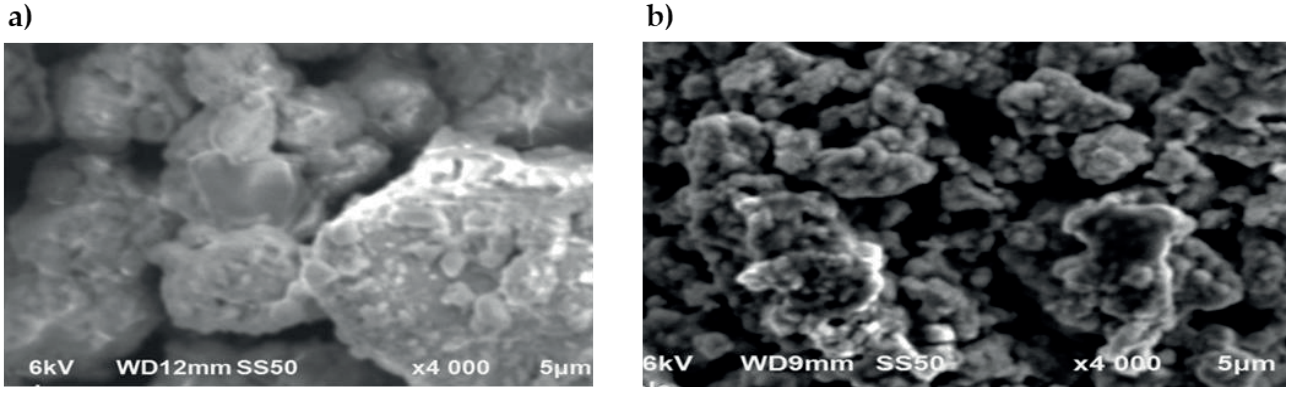


Figure 2. SEM images of (a) unmodified Fe_3O_4 nanoparticles, and (b) Fe_3O_4 nanoparticles modified with *M. oleifera* seed protein extract (reproduced from Amuanyena et al. 2019[20] with permission).

Similarly, Padmavathy et al.[19] employed TGA to evaluate Fe_3O_4 nanoparticles used for Cr(VI) removal. The steady weight loss up to nearly 200 °C was linked to the removal of moisture, whereas persisted mass loss at higher temperatures displayed thermal degradation of species linked to the surface. The complete decomposition of labile surface constituents was confirmed by stabilisation of mass above 600 °C, exhibiting information on the stability of the material during practical applications.

Enhanced sensitivity for functionalised adsorbents' thermal activities is provided by TGA combined with derivative thermogravimetric analysis (DTGA). TGADTGA was employed by Ihsanullah et al.[31] to acidmodified AC and CNTs. In acidmodified CNTs, the presence of lowtemperature decomposition peaks verified the establishment of thermally unstable functional groups containing oxygen after acid treatment. For modified AC, DTGA displayed the elimination of amorphous carbon and volatile impurities, resulting in a more thermally stable and purer surface. Successful chemical modification and enhanced surface characteristics appropriate to adsorption are directly verified by these observations.

Generally, TGA and DTGA are vital tools for verifying functionalisation by detecting further decomposition stages, evaluating the thermal stability, assessing the relative loading of organic modifiers, and are associated with surfacebound functional groups of modified adsorbents.

Fourier transform infrared spectroscopy

Fourier transform infrared spectroscopy (FTIR) is a key technique for confirming successful surface functionalisation of adsorbents, as it identifies the functional groups present on a material and provides information on the nature and strength of chemical bonding.[23] Functionalisation is verified by the appearance of new vibrational bands, changes in band intensity, or shifts in peak positions relative to the unmodified material, which indicate the introduction of organic modifiers or interactions between functional groups and the adsorbent surface. FTIR operates by measuring the absorption of infrared radiation by molecular vibrations within a sample. The resulting spectra, typically collected between 400 and 4000 cm^{-1}, reflect characteristic stretching and bending modes of chemical bonds. In functionalised materials, comparison of spectra before and after modification enables direct confirmation of surfacebound functional groups, while spectral changes after adsorption provide insight into metal–ligand interactions. This approach is illustrated by Mihăilescu et al.,[33] (Figure 5) who used FTIR spectroscopy to confirm the successful functionalisation of Amberlite XAD7 resin with Lglutamic acid for Au(III) recovery. The modified resin exhibited characteristic absorption bands corresponding to aminoacid functional groups, including amide $–NH_2$ stretching at 3 540 cm^{-1}, broad hydroxyl (–OH) stretching at approximately 3 000 cm^{-1}, carbonyl (C=O) stretching at 1 641 cm^{-1}, and free amine (–NH–) vibrations at 1 579 and 1 559 cm^{-1}. Additional C–O stretching bands at 1 317 and 1 151 cm^{-1} further confirmed the presence of glutamicacidderived functionalities. The appearance of these bands, which are absent in the unmodified resin, provides direct evidence of successful surface functionalisation. These

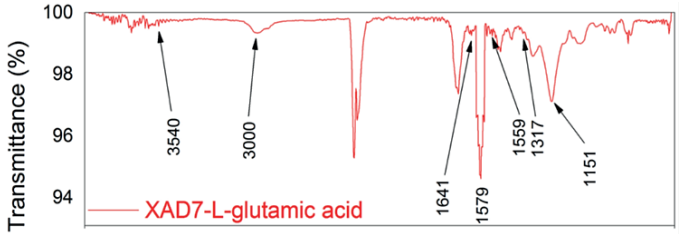


Figure 5. FTIR spectrum of Amberlite XAD7 resin modified with L-glutamic acid (reproduced from Mihăilescu et al. 2019[33] with permission).

functional groups play a key role in Au(III) adsorption through electrostatic attraction and coordination interactions, thereby linking FTIR spectral features directly to adsorption performance.

Similarly, Iqbal et al.[34] confirmed the functionalisation of magnetic multiwalled carbon nanotubes (MWCNTs) through the appearance of characteristic FTIR bands at 3 400 cm^{-1} (–OH stretching), 2 920 cm^{-1} (aliphatic C–H stretching), 1 620 cm^{-1} (C=C stretching of alkenes), and 1 470 cm^{-1} (C=O stretching). These oxygen and carboncontaining functional groups are introduced during oxidation and modification processes and are responsible for enhanced interaction with preciousmetal ions, confirming the success of the functionalisation strategy.

Egbosiuba et al.[26] further demonstrated the utility of FTIR in verifying both functionalisation and adsorption mechanisms for MWCNTs decorated with greensynthesised Ag nanoparticles (MWCNTsKIAgNPs). Before adsorption, FTIR spectra showed C–H bending and stretching vibrations at 2 835 and 895 cm^{-1}, C–C vibrations at 1 959 cm^{-1}, and multiple carbonyl (C=O) bands at 2 114, 2 365, and 1 250 cm^{-1}, confirming the presence of aliphatic, aromatic, and oxygencontaining functional groups. Additional O–H and C–O stretching bands at 3 000 cm^{-1} and 1 078 cm^{-1}, respectively, indicated hydroxyl and carboxylic functionalities, while a strong hydroxyl stretching band appeared at 3 680 cm^{-1}. Notably, bands at 3 890 cm^{-1} (overlapping –OH/$–NH_2$/–NH– stretching) and 704 cm^{-1} (C–H bending of alkenes) disappeared after adsorption, providing direct evidence that these functional groups participated in heavymetal binding.

Mohamed Khalith et al.[35] used FTIR to confirm biomoleculeassisted functionalisation of Fe_3O_4 nanoparticles synthesised using orange peel extract (OPE). Characteristic bands at 3 312 cm^{-1} (–OH stretching), 2 358 cm^{-1} ($–NH_2$), 2 120 cm^{-1} (–C≡CH), and 1 635 cm^{-1} (C–H bending) confirmed the presence of plantderived organic functional groups on the nanoparticle surface. Etherrelated bands at 1 010 cm^{-1} and 1 097 cm^{-1} further supported successful functionalisation. Importantly, systematic shifts of the –OH, $–NH_2$, and –C≡CH bands to higher wavenumbers after modification provided strong evidence of chemical interactions between OPE components and Fe_3O_4. The integrity of the magnetic core is confirmed by the Fe–O stretching vibrations observed at 435 and 535 cm^{-1}.

Generally, FTIR spectroscopy verifies successful functionalisation by sensing peak changes related to chemical interactions, identifying newly presented functional groups at definite wavenumbers, and revealing the participation of these groups in PMs and Cr(VI) adsorption. This makes FTIR an essential tool for linking surface chemistry modification to adsorption performance in functionalised adsorbents.

Brunauer-Emmett-Teller (BET) method

This technique evaluates the successful functionalisation of adsorbents by measuring porosity, specific surface area, and provides textural evidence, including total accessible surface area, changes in pore volume, and average pore size.[23] These exhibit structural changes caused by the introduction of chemical treatments, functional groups, or nanoparticles. These measurable shifts serve as indirect but consistent values of effective functionalisation.

To remove adsorbed impurities and moisture, confirming full availability of pores during nitrogen adsorption before degassing of materials at high temperatures is required. For instance, Anyika et al.[16] employed degassing for an hour at 90 °C, followed by 4 h at 350 °C to make sure that nitrogen could access all pore structures. This aids in correct surface area calculation and isotherm generation. Functionalisation tends to naturally change the textural appearances of adsorbent materials in predictable ways. Reduced pore volume or surface area signifies effective deposition of nanoparticles or functional groups within pores, partially coating the surface or blocking them.

Formation of new pores or improved surface area reveals chemical treatments that introduce new surface defects, open existing pores, or prevent particle aggregation. Changes in the distribution of pore size imply reorganisation or rearrangement of the carbon matrix owing to functionalisation chemistry. The key indication that surface modification has happened is provided by these BETderived variations even before adsorption studies. This theory is supported constantly by numerous studies. BET to magnetic Fe_3O_4/Mg–Al layered double hydroxide nanocomposites was applied by Biata et al.[22] and obtained improved porosity and surface area after functionalisation, which is associated with the creation of further pore structures that enhanced accessibility for PMs. Functionalisation of MWCNTs with silver nanoparticles was confirmed by a decrease in specific surface area from 1 250 to 1 236 m^2/g in a similar study by Egbosiuba et al.[31] This is associated with fractional pore obstruction of the nanoparticles attached, and this reduction promptly confirmed that decoration with KIAgNPs had happened.

Lastly, BET was used by Ihsanullah et al.[31] to assess acidmodified CNTs and AC, obtaining significant surface area values of 1 420 m^2/g and 170 m^2/g, respectively. The intense increase compared to unmodified materials signaled effective surface cleaning and pore opening caused by acid treatment.

Overall, these results highlight the significant role played by BET analysis in verifying effective functionalisation by detecting expected, measurable variations to the material's surface porosity and texture. BET offers vigorous justification that chemical modification has changed the adsorbent in ways consistent with enhanced performance.

Vibrating sample magnetometry (VSM)

This technique confirms successful functionalisation of magnetic adsorbents since surface modification directly varies these key magnetic parameters, namely coercivity, hysteresis behaviour, saturation magnetisation (M_s), and remanent magnetisation (M_r).[23] When a functional layer, such as metal nanoparticles, polymers, biomolecules, or carbonaceous materials, is integrated onto a magnetic core such as Fe_3O_4, it classically decreases or moves the material's magnetic response due to modification of surface spin alignment, dilution of the magnetic phase, or changes in particle size. Thus, predictable changes in the magnetic signature provide strong indirect evidence of successful functionalisation.

Mourdikoudis et al.,[23] stated that VSM yields magnetisation–field (M–H) hysteresis loops, from which coercivity, M_s, and M_r values are obtained. Effective functionalisation is usually verified when the M–H curve shows: Suppressed hysteresis (superparamagnetic behaviour), demonstrating establishment of smaller, surfacemodified magnetic domains, reduced M_s, representing coating of non-magnetic nanoparticles with magnetic material, and deviations in coercivity, signalling changed magnetic anisotropy due to surface change. This trend is steadily exhibited throughout studies utilising magnetic adsorbents for wastewater treatment. Significant decline in magnetisation from 34 emu/g for unmodified Fe_3O_4 to 22 emu/g for the Fe_3O_4–oMWCNT composite confirmed functionalisation of Fe_3O_4 with oxidised multiwalled carbon nanotubes (oMWCNTs) in the work by Iqbal et al.34 This decrease supports the existence of a nonmagnetic carbon layer covering the Fe_3O_4 particles, thereby verifying effective integration of CNTs into the composite.

Mohamed Khalith et al.,[35] observed a similar trend when using agricultural waste-derived carbon to synthesise magnetite carbon nanocomposites. A progressive decrease in M_s from 0.17 emu/g for Fe_3O_4 nanoparticles, to 0.04 emu/g for the highly porous carbon (HPC), and further down to 0.0025 emu/g for the entirely functionalised GMC composite was shown by their VSM measurements. Superparamagnetic behaviour, which is consistent with effective reduction and surface coating of magnetic domain sizes upon functionalisation, is confirmed by the absence of detectable M_r and negligible coercivity values (110, 55, and 0 Oe, respectively). Regardless of the decreased magnetisation, the materials were still easily separable with an external magnet, proving that functionalisation sustained magnetic responsiveness essential for practical recovery.

The use of VSM was also demonstrated by Mittal,[27] confirming the functionalisation of mesoporous Fe_3O_4 nanoparticles. The M_s value of 46.213 emu/g displayed the great magnetic content representative of surfacemodified but structurally intact Fe_3O_4, while the Sshaped hysteresis loop with no noticeable remanence implied superparamagnetism. The capability to magnetically separate the nanoparticles from aqueous solution at this M_s further verified that functionalisation did not compromise operational magnetic properties.

Overall, these results demonstrate that VSM displays more than magnetic properties: shifts in hysteresis shape, M_s, coercivity, and M_r act as consistent indicators of effective functionalisation. The direction and degree of these variations are linked to the magnitude and category of surface modification, making VSM an essential tool for justifying magnetic nanocomposites utilised in Cr(VI) removal and PMs recovery.

ADSORPTION STUDIES

The effectiveness of functionalised adsorbents is managed by numerous operational parameters, namely contact time, pH, initial metalion concentration, temperature, and adsorbent dosage. For optimising systems constructed for the recovery or removal of PMs and Cr(VI) from aqueous media, a good understanding of how these variables impact adsorption performance is fundamental. To accomplish this, kinetic analyses and adsorption isotherms are necessary. Kinetic studies reveal the rate at which adsorption happens and find the processes that influence mass transfer and surface interactions, whereas isotherm models define the connection between the quantity reserved on the adsorbent surface and equilibrium concentration of the adsorbate in solution, offering insight into adsorption mechanisms and surface characteristics. Overall, these evaluations form the systematic foundation for assessing and improving the performance of functionalised adsorbents in wastewater remediation applications.

Adsorption from solution

For PMs stock solutions, chloride salts were dissolved in distilled water and diluted further to the required working solutions in the study by Amuanyena et al.[20] To obtain preferred basic or acidic conditions, dilute sodium hydroxide or hydrochloric acid was used. Centrifuge tubes with prepared adsorbent and metal solutions of platinum(IV), palladium(II), and gold(III) were used to conduct batch adsorption experiments. The mechanical shaker was used to shake the solution at 150 rpm, allowed to settle, filtered, and the concentrations of metals remaining in the solution were measured using the Inductively Coupled Plasma Optical Emission Spectroscopy (ICP-OES). Potassium dichromate was used for chromium(VI), the same procedure as for PMs was used to prepare the stock solution, a UV–Visible spectrophotometer calibrated at the optimum analytical wavelength was used to determine Cr(VI) concentrations.[26,36]

Optimal adsorption conditions were determined by systematically varying key experimental variables, namely adsorbent dosage, agitation time, pH, and initial adsorbate concentration. Triplicate analyses were performed for all measurements and recorded as mean values. Equations (1) and (2) were used to calculate the recovery efficiency at equilibrium (%R):

$$\%R = \frac{C_i - C_f}{C_i} \times 100 \quad (1)$$

and the equilibrium adsorption capacity (q_e):

$$q_e\,(mg/g) = \frac{V(C_o - C_f)}{m} \quad (2)$$

where C_o or C_i is the initial metal adsorbate concentration (mg/L), C_f is the final concentration (mg/L), m is the mass of the adsorbent (g), and V is the volume of the solution (L). Unknown concentrations based on instrument response were calculated from calibration curves obtained from standard dilutions. The used adsorbent was recycled with a suitable solvent to allow further reuse or evaluation after adsorption.

Adsorbent dosage

Adsorbent dosage is a significantly effective variable in batch adsorption systems, as it clearly establishes the number of vacant binding sites accessible for interaction with the target PMs and Cr(VI). Changing the adsorbent dosage and keeping the initial concentration, contact time, temperature, and pH constant allows for the evaluation of how adjustments in the solidtoliquid ratio affect adsorption capacity and removal efficiency. Determining the optimum dosage is consequently fundamental for guaranteeing efficient utilisation of the adsorbent while preventing excessive material input or decreased performance caused by particle aggregation or oversaturation.

Amuanyena et al. [20] (Figure 6) evaluated the effect of adsorbent dosage on the recovery of precious metals using Fe_3O_4 nanoparticles functionalised with Moringa oleifera seed proteins. The dosage was varied between 0.005 and 0.085 g, at pH 2.5, an equilibrium time of 120 min, and an initial concentration of 10 mg L^{-1}. Recovery increased with increasing dosage up to an optimum of 0.065 g, beyond which a decline was observed. At the optimum level, the percentage recoveries were 99.8% for Au(III), 87.7% for Pd(II), and 72.7% for Pt(IV). The decline beyond the optimum dosage was attributed to a reduction in the number of vacant active sites relative to the available PMs, consistent with the saturation of adsorption sites and reduced adsorption efficiency when excess adsorbent is present.

Similarly, Iqbal et al.[34] investigated the dosage effect for Fe_3O_4–oxidised multiwalled carbon nanotube (oMWCNT) composites over a range of 2–16 mg. Removal efficiency increased steadily until reaching an optimum at 10 mg, after which no further improvement was achieved. A decreased ratio of adsorbate to vacant surface sites and particle aggregation, causing reduced adsorption capacity and lower efficient surface area, explained the plateau and subsequent decrease at higher dosages.

A wider dosage range (25–250 mg) applying acidmodified AC and CNTs for the remediation of Cr(VI) was explored by Ihsanullah et al.[33] Modified AC yielded 99% Cr(VI) removal at an optimum dosage of 75 mg, thereafter removal declined because of site saturation. Conversely, modified CNTs achieved an 87% removal with a substantially higher optimum dosage of 175 mg, an improvement relative to the 80% removal using 150 mg obtained for raw CNTs. An acid treatment introduced additional active sites, which boosted adsorption affinity and surface functionality, hence enhancing the performance of modified CNTs.

A constant pattern appears across the three studies: Removal efficiency is improved with a rise in adsorbent dosage till an optimum level is obtained, thereafter performance declines or becomes constant. Different specific optimum dosages are obtained for these materials: Fe_3O_4 modified with Moringa 0.065g, Fe_3O_4–oMWCNT composites 10 mg, modified AC 75 mg, and modified CNTs 175 associated with differences in adsorbent–adsorbate affinity, surface area, and functionalisation. Materials with larger heterogeneity or lesser site availability require higher dosages, whereas those with greater surface functionality or higher activesite density require lower dosages to attain greater recovery. For all these, dosages beyond the optimum result in imbalanced adsorbent to adsorbate ratios, decreased active surface area, and reduced performance resulting from aggregation. This demonstrates that optimum dosage is both adsorbentspecific and intimately linked to physicochemical surface characteristics governing adsorption behaviour.

pH

pH is a key factor governing adsorption behaviour because it influences both the surface charge of the adsorbent and the chemical speciation of metal ions in solutions. During pH-dependent studies, all other parameters, namely contact time, temperature, adsorbent dosage, and initial metalion concentration, are kept constant, while dilute HCl or NaOH is used to achieve the desired pH range.

Mihăilescu et al.,[33] (Figure 7) examined the adsorption of Au(III) onto Amberlite XAD7 modified with Lglutamic acid across pH 2–14 under fixed conditions (0.1 g adsorbent, 25 °C, 60 min agitation, 5 mg L^{-1} Au(III)). Adsorption was highest at pH < 4, followed by a sharp decrease as pH increased. This behaviour resulted from the formation of negatively charged $[AuCl_4]^-$ complexes in acidic media, which interact strongly with protonated $-NH_3^+$ groups on the modified resin. Decreased electrostatic attraction and the amine groups' deprotonation are associated with adsorption approaching zero at pH > 8.

For the adsorption of Ru(III), Pt(IV), and Pd(II) using ChitosanDB18C6, comparable pH-dependent trends were reported by Grad et al[37] At pH < 3**,** PMs exist primarily as negatively charged chlorometalate complexes ($[RuCl_4]^-$, $([PtCl_6]^{2-}$, $[PdCl_4]^{2-}$) and maximum capacities were observed. The interaction between protonated amine groups and these PMs on chitosan resulted in high adsorption, whereas adsorption decreased promptly as the density of protonated surface sites declined and pH increased.

The effects of pH were further explored by Egbosiuba et al.[18] for the adsorption of Ni(II), Cd(II), Fe(II) and Cr(VI) onto MWCNTs–KIAgNPs. Maximum capacities of 218.32 mg g^{-1} Ni(II), 83.20 mg g^{-1} Cd(II), and 133.63 mg g^{-1} Fe(II) were recorded at pH 6, whereas

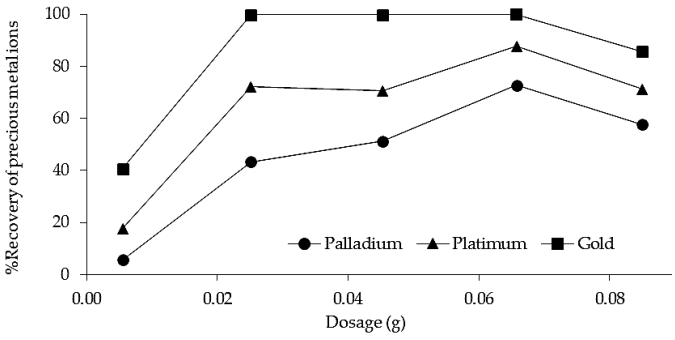


Figure 6. The effect of dosage on the recovery of precious metal ions using magnetic iron oxide nanoparticles modified with *M.oleifera* seed protein extract (reproduced from Amuanyena et al. 2019[20]with permission).

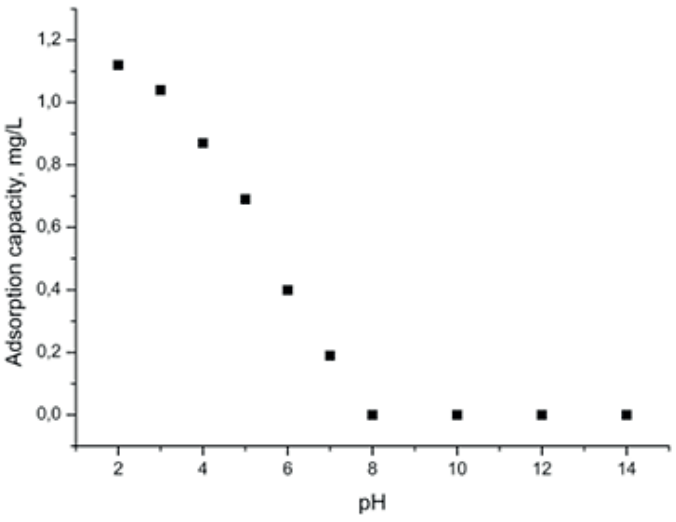


Figure 7. Influence of pH on the recovery of Au(III) with Amberlite XAD7 resin modified with L-glutamic acid (reproduced from Mihăilescu et al. 2019[33] with permission).

Cr(VI) exhibited its highest capacity (298.12 mg g^{-1}) at pH 3. Based on the study, numerous oxyanion forms, namely $HCrO_4^-$, CrO_4^{2-}, $Cr_2O_7^{2-}$, exist for Cr(VI) and their dominance depends greatly on pH. The dominant species becomes CrO_4^{2-} at higher pH, which is repelled by the negatively charged surface of the composite (pH > 6), resulting in a reduction in adsorption. The abundant species are $Cr_2O_7^{2-}$ and $HCrO_4^-$ at low pH which strongly attract the positively charged surface of the nanocomposite, leading to high removal of Cr(VI). The competition between excess H^+ ions and Ni(II), Cd(II), and Fe(II) for vacant active sites resulted in diminished adsorption observed in strongly acidic environments. The point of zero charge (pHpzc) of the composite was reported as pH 6, suggesting a negatively charged surface at pH > 6 and a positively charged surface at pH < 6, which agrees with the adsorption behaviour observed.

The significance of surface charge was similarly emphasised by Mittal et al.[27] obtaining a pHpzc value of **2.52** for the remediation of Cr(VI) using greensynthesised mesoporous Fe_2O_3 nanoparticles. This low value for pHpzc implies that the material has a positive charge in strongly acidic environments, encouraging electrostatic attraction with oxyanions of Cr(VI) and improving removal effectiveness.

The effect of pH for Cr(VI) removal between pH 2–8 using acidmodified AC and CNTs was also explored by Ihsanullah *et al.*[31] Modified CNTs and AC showed the highest removal at pH 3-4, whereas modified AC performed optimally at pH 3. The authors associated this with the dominance of $Cr_2O_7^{2-}$ and $HCrO_4^-$ when pH is low, which all adsorb effectively on positively charged surfaces. On the other hand, CrO_4^{2-} predominates at higher pH levels and may experience electrostatic repulsion or undergo precipitation as $Cr(OH)_3$, which all decrease removal effectiveness.

In all studies, optimal adsorption of metal ions, especially PMs chlorocomplexes and Cr(VI) oxyanions, appears in acidic conditions where favourable electrostatic interactions dominate since adsorbent surfaces are positively charged. Whereas the specific optimal pH differs between adsorbents due to variations in surface chemistry, isoelectric point, and functional groups, a constant decrease in performance is reported as pH rises and either electrostatic repulsion or deprotonation occurs. This behaviour is further influenced by changes in oxyanion speciation for Cr(VI), with $Cr_2O_7^{2-}$ and $HCrO_4^-$ favouring adsorption at minimal pH and CrO_4^{2-} contributing to diminished removal at high pH. These results mutually highlight the central role of pH in modulating both metalion speciation and adsorbent surface charge, thus influencing adsorption effectiveness across various materials.

Temperature

This is a vital parameter affecting adsorption, as it can influence the energetics of binding interactions, diffusion into pores, and adsorbate mobility. During temperature-dependent studies, all other operational conditions, namely initial metal ion concentration, pH, adsorbent dosage, and contact time, are maintained constant, while the solution is agitated uniformly.

Mihăilescu et al.[33] investigated the recovery of Au(III) using Amberlite XAD7 modified with Lglutamic acid across 25–45 °C. Although adsorption increased slightly with temperature, the effect was reported to be minimal, and 25 °C was identified as the optimal temperature, indicating that raising the temperature did not provide meaningful gains in adsorption capacity and would therefore not be economically beneficial for practical applications. The authors attributed the adsorbent's performance mainly to its high specific surface area, which already provided sufficient active sites under ambient conditions.

A related trend was observed by Grad et al.[37] for ChitosanDB18C6 in the adsorption of Pt(IV), Pd(II), and Ru(III). Using a similar temperature range (25–45 °C), the authors reported that higher temperatures enhanced adsorption, indicating that the processes studied were endothermic. The observed rise may be linked to increased accessibility of vacant sites or enhanced diffusion of PMs at higher temperatures.

The effects of temperature were evaluated by Mohamed Khalith et al.[35] using Fe_3O_4 carbon nanocomposites synthesised from agricultural by-products for the remediation of Cr(VI). The removal efficiency increased reasonably from 85.1% to 86.2% until 55 °C when the temperature was varied between 35 and 75 °C. After which, removal was constant at 65 °C, then decreased to 85.7% at 75 °C, implying that the structure of the adsorbent surface may be altered by exposure to higher temperatures and lower its capacity.

In all the studies reviewed, temperature explains a materialspecific impact on adsorption behaviour. For instance, techniques like Amberlite XAD7–Lglutamic acid, optimal performance was already reached at ambient conditions, hence temperature shows little practical benefit. Conversely, at higher temperatures, ChitosanDB18C6 exhibited an enhanced adsorption, consistent with an endothermic process. Insignificant improvement at moderate temperatures, followed by a decrease at higher temperatures that may indicate changes to the adsorbent surface, was exhibited by Cr(VI) adsorption on Fe_3O_4 carbon composites. Together, these results show that while temperature can impact adsorption performance, the magnitude and direction of its outcomes depend strongly on the thermodynamic characteristics, functionalisation, and structural stability of the specific adsorbent system.

Contact time

In batch adsorption studies, contact time is a key effective parameter as it determines the period during which adsorbate species interact with vacant active sites on the adsorbent surface. During these studies, the solution is mixed at a fixed rate to ensure uniform mixing, and variables, namely adsorbent dosage, initial concentration, temperature, and pH, are fixed. The time required to reach adsorption equilibrium, after which no substantial differences in removal effectiveness are observed, is obtained by taking measurements at specified intervals.

As shown in Figure 8, the adsorption of Au(III) onto Amberlite XAD7 modified with Lglutamic acid between 20–120 min was examined by Mihăilescu et al.[33] A steady increase in adsorption capacity was observed till an equilibrium time of 60 min, after which no further increase happened. At equilibrium, the adsorption capacity was reported as 1.2 mg g^{-1}, indicating that most active sites had become occupied within the first hour of treatment.

For the adsorption of Ru(III), Pt(IV), and Pd(II) on ChitosanDB18C6, a comparable trend was reported by Grad et al.[37] For this, adsorption escalated gradually with contact time till an optimum of 180 min was

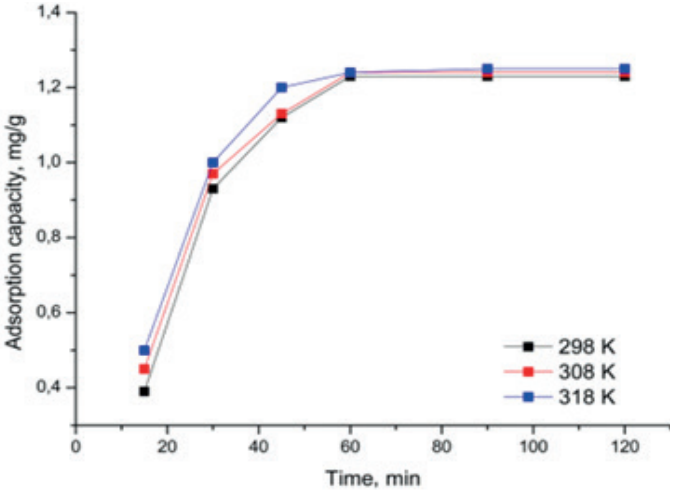


Figure 8. Effects of contact time and temperature on the recovery of gold(III) using Amberlite XAD7 resin-L-glutamic acid (reproduced from Mihăilescu et al. 2019[33] with permission).

reached. Beyond 180 min, the adsorption capacity for all three PMs remained essentially unchanged, and this time was subsequently used for all further experiments.

The effect of contact time over a wider range between 30–450 min for PM extraction from e-waste using Fe_3O_4–oMWCNT composites was investigated by Iqbal et al.[34] Their findings agreed with those of Grad et al.[37], indicating that adsorption capacity increased as contact time increased until 180 min, beyond which equilibrium was obtained. The authors associated the primary increase with many vacant active sites and the later plateau with the gradual saturation of these sites.

The effect of contact time on the adsorption of Cr(VI) with acidmodified CNTs and modified AC under fixed conditions (pH 3, 1 mg L^{-1} Cr(VI), 200 rpm, and 50 mg adsorbent) was evaluated by Ihsanullah et al.[31] The equilibrium was reached quicker, at 2 h, for modified CNTs, suggesting that though CNTs took a longer time to reach similar removal before modification, functionalisation of the surface substantially enhanced their adsorption rate. Equilibrium was attained at 4 h for modified AC, with a maximum removal of 98%. The authors associated the high removal effectiveness with the improved availability of vacant active sites and widened surface area produced by acid treatment.

For all the studies reviewed, contact time impacts adsorption until equilibrium is attained, beyond which further increases result in no significant enhancement in removal. Although the exact equilibrium time differs by adsorbent category and material characteristics, 4 h for modified AC, 2 h for modified CNTs, 180 min for Fe_3O_4–oMWCNT and ChitosanDB18C6 composites, 60 min for modified Amberlite XAD7, the pattern overall is maintained. Materials with improved porosity or greater surface functionality tend to attain equilibrium faster, while those with complex surface structures or more heterogeneous require lengthier contact times. The trend throughout studies suggests that equilibrium contact time principally reveals the interplay between the strength of adsorbent–adsorbate interactions, the rate of diffusion into surface pores, and the number of available active sites.

Initial metal ion concentration

The parameter that plays an important role in determining adsorption performance, as it impacts the driving force for mass transfer between the adsorbent surface and solution, is the initial concentration of metal ions. These experiments are conducted at varied initial metal ion concentrations and fixed pH, temperature, adsorbent dosage, and contact time. The point at which adsorbent surface sites become saturated is obtained by examining adsorption capacity and removal efficiency across these concentrations.

A range of initial concentrations was used by Mihăilescu et al.[33] (Figure 9) to examine the adsorption of Au(III) on Amberlite XAD7 modified with Lglutamic acid, whereby adsorption capacity improved with an increase in concentration till an optimum of 75 mg L^{-1} was attained. The maximum adsorption capacity was 14.23 mg g^{-1} at this concentration, after which no further rise was observed. This plateau implies that the vacant surface sites were fully occupied at higher concentrations, preventing additional adsorption.

ChitosanDB18C6 was used by Grad et al.[37] for the adsorption of Pd(II), Pt(IV) and Ru(III), a similar trend was reported. Maximum adsorption capacities of 17.6 mg g^{-1}, 22.6 mg g^{-1}, and 30.4 mg g^{-1}, respectively, with corresponding optimal initial concentrations of 175 mg L^{-1} for Pt(IV), 150 mg L^{-1} for Pd(II), and 175 mg L^{-1} for Ru(III), were obtained. For all three metals, adsorption capacity initially increased but remained constant at higher concentrations, implying that saturation of active sites reduced further uptake.

Cr(VI) adsorption with several agricultural by-products at initial concentrations between 25 and 400 mg L^{-1} was investigated by El-Baz et al.[38] The study found that removal effectiveness decreased, although adsorption capacity increased with initial concentration. The optimal initial concentration was 25 mg L^{-1} for Cr(VI), where removal effectiveness were 48% for both sugarcane bagasse and Phragmites australis, and 76% for sawdust and 84% for banana waste. The rapid saturation of the restricted active sites on the lowcost biosorbents was associated with the decrease in removal effectiveness at higher concentrations.

Cr(VI) adsorption with a greensynthesised Fe_3O_4 carbon nanocomposite at five different initial concentrations (30.41, 24.3, 18.24, 12.16, and 6.08 mg L^{-1}) was also examined by Mohamed Khalith et al.[35] High removal between 99.3% to 100% was reported for all concentrations, indicating that the adsorbent retained an abundance of active sites able to sustain monolayer adsorption also at high concentrations.

For all studies, initial metal ion concentration illustrates an evident effect on adsorption behaviour, with adsorption capacity largely increasing as concentration rises, up to a saturation point. Each adsorbent has a different specific concentration at which saturation happens: 25 mg L^{-1} for agricultural residues, up to 30.41 mg L^{-1} for Fe_3O_4 carbon nanocomposites, 75 mg L^{-1} for Amberlite XAD7–Lglutamic acid, and 150–175 mg L^{-1} for ChitosanDB18C6 without a distinct decrease in removal. These variations exhibit the availability of active sites and changing density across adsorbent types. Whilst biosorbents with lesser surface functionality experience saturation faster, chemically modified materials and functionalised nanocomposites sustain great removal across a larger range of concentrations. In all, initial adsorbate concentration functions as a fundamental determining factor of adsorption capacity and emphasises the importance of matching adsorbent characteristics to the concentration levels estimated in real wastewater systems.

Competitive adsorption and selectivity

Functional groups existing on the adsorbent surface, competing ions, and chemical environment repeatedly influence selectivity in adsorption systems. PMs typically form definite chlorocomplexes under acidic conditions, which may interact differently with protonated functional groups, as reported in various studies reviewed here. For instance, at low pH, Lglutamic acid modified Amberlite XAD7 forms protonated $-NH_3^+$ groups that readily adsorb negatively charged $[AuCl_4]^-$ complexes formed from Au(III), as reported by Mihăilescu et al.,[33] indicating extensive selectivity in acidic conditions. Correspondingly, Grad et al.[39] reported that at low pH, anionic chloride complexes formed from Pd(II), Ru(III), and Pt(IV) were favorably attracted to protonated chitosanbased material, with competitive adsorption declining as chloride activity decreased and fewer complexes formed.

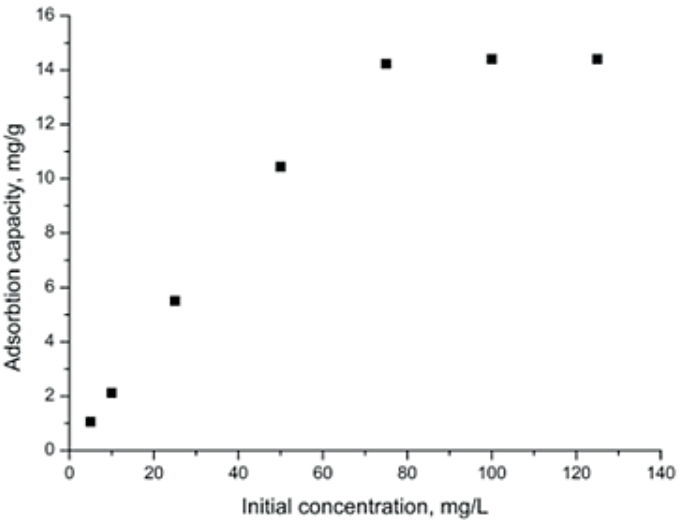


Figure 9. Effect of the initial adsorbate on the recovery of gold(III) using Amberlite XAD7-L-glutamic acid (reproduced from Mihăilescu et al. 2019[33] with permission).

The zetapotential studies also highlighted that competitive adsorption is strongly affected by the surface charge of the adsorbent. At higher pH, modified Fe_3O_4 nanoparticles became progressively negatively charged, decreasing affinity for anionic species while increasing competition from cationic species under specific conditions. The study emphasised that pHdependent surface charge changes may suppress or favour specific ions when diverse species coexist in solution, implying that selectivity may be dynamic rather than fixed. Similarly, for MWCNTsKIAgNPs, Egbosiuba et al.[18] demonstrated that Cr(VI) removal was strongly preferred at low pH due to dominance of $HCrO_4^-$, whilst competitive adsorption with Ni(II), Fe(II) and Cd(II) improved at higher pH where anion affinity was reduced by surface deprotonation, demonstrating that solution structure can change selectivity patterns significantly. Kinetic behaviour and adsorptionisotherm may further provide evidence of competitive interactions. For example, Fe_3O_4oMWCNT composites exhibited high selectivity toward Au(III), Ag(I), and Pd(II) despite the presence of other metal ions as reported by Iqbal et al.[34], with Langmuirtype monolayer uptake indicating occupation of highly specific surface sites. Significant selectivity of Fe_3O_4/MgAlLDH nanocomposites toward Ir(IV) and Au(III) was also retained, as reported by Biata et al.,[22] where pseudosecondorder kinetics supported strong chemisorptive interactions that appeared to prevail even with competing species existing, demonstrating that functionalisation may improve preferential binding affinities.

Steric constraint or pore blockage, specifically in systems where various metal ions interact with heterogeneous natural materials, may also demonstrate competitive. In this regard, simultaneous uptake of various PM ions was demonstrated by pomegranatepeelderived biosorbents, as reported by Zhu et al.[30] and their SEM–EDS mapping verified the presence of multiple adsorbed species following multiion exposure. These findings suggest that natural biosorbents may contain a variety of functional sites with differing affinities, which could contribute to competitive binding under mixedmetal conditions.

Overall, the literature incorporated in this review suggests that selectivity and competitive adsorption may depend on multiple interrelated factors, including surface functionalisation, metalcomplex speciation, pHdependent charge behaviour, steric constraints, and the presence of competing ions. These findings collectively indicate that although many functionalised adsorbents display promising selectivity patterns, the adsorption environment may substantially influence competitive interactions, and future work optimising solution chemistry and surface modification may further enhance selectivity under real wastewater conditions.

ADSORPTION ISOTHERMS, KINETICS, AND THERMODYNAMICS

Adsorption isotherms for evaluation of equilibrium conditions

Adsorption isotherms describe how adsorbate molecules distribute between the liquid and solid phases at equilibrium.[39] Among the widely used models, the Langmuir and the Freundlich isotherms are the most common. Linear regression of the isotherm data provides a coefficient of determination (R^2), where values approaching 1 indicate a stronger fit of the model to the experimental data.

Langmuir isotherm model

The Langmuir isotherm assumes monolayer adsorption on a homogeneous surface, where all adsorption sites possess equal affinity for the adsorbate, and no interactions occur between adsorbed molecules.[36,38] Under constant adsorption energy, adsorption increases until a saturated monolayer is formed, after which no further adsorption can occur. The linearised Langmuir equation is:

$$\frac{C_e}{q_e} = \frac{1}{bq_m} + \frac{C_e}{q_m} \quad (3)$$

where: q_m (mg g^{-1}) is the maximum monolayer adsorption capacity, b is the Langmuir constant, q_e (mg g^{-1}) is the adsorption capacity at equilibrium, and C_e (mg L^{-1}) is the equilibrium adsorbate concentration.A straight line obtained from a plot of C_e versus C_e/q_m confirms Langmuir behaviour. The favourability of adsorption is assessed using the separation factor R_L:

$$R_L = \frac{1}{1 + bC_o} \quad (4)$$

Interpretation of R_L: $R_L < 1$: favourable adsorption; $R_L > 1$: unfavourable adsorption; $R_L = 1$: linear adsorption and $R_L = 0$: irreversible adsorption

Freundlich isotherm model

The Freundlich isotherm describes multilayer adsorption on heterogeneous surfaces with non-uniform distribution of adsorption energies.[36,38] The linear form of the equation is:

$$\log q_e = \log K_F + 1/n \log C_e \text{ or } \ln q_e = \ln K_F + 1/n \ln C_e \quad (5)$$

where: K_F indicates adsorption capacity (higher values reflect stronger adsorption), 1/n represents surface heterogeneity.

Interpretation of 1/n: $1/n < 1$: normal adsorption and $1/n > 1$: cooperative adsorption.

Sips isotherm model

The Sips isotherm, also known as the Langmuir–Freundlich model, merges both models to describe adsorption on heterogeneous surfaces at low concentrations while approaching Langmuir behaviour at high concentrations.[40] The general form is:

$$q_e = \frac{q_{ms} K_s C_e^{ns}}{1 + K C_e^{ns}} \quad (6)$$

with: q_{ms} (mg g^{-1}) maximum adsorption capacity, K_s (L mg^{-1}) Sips equilibrium constant, and n_s Sips exponent indicating system heterogeneity.

Model behaviour: At low C_e and $n_s = 1$, behaves like Freundlich, and at high C_e and $n_s = 1$, behaves like Langmuir.

A value of $1/n_s > 1$ suggests greater heterogeneity, whereas $1/n_s \approx 1$ indicates more homogeneous adsorption sites.

Temkin isotherm model

The Temkin isotherm accounts for adsorbent–adsorbate interactions and assumes that the heat of adsorption decreases linearly with surface coverage.[38] The linear form is:

$$qe = B \ln KT + B \ln Ce \quad (7)$$

where: B is related to the heat of adsorption and K_T is the equilibrium binding constant.

This model is particularly useful for understanding systems where adsorbent–adsorbate interactions play a significant role.

Dubinin-Radushkevich (D-R)

The D–R isotherm is derived from Polanyi's theory of adsorption potential and is applied to distinguish between physical and chemical adsorption based on mean adsorption energy potential.[40] It is expressed as:

$$q_e = q_{mDR} e^{-K_{DR}\varepsilon^2} \quad (8)$$

with the adsorption potential ε defined as:

$$\varepsilon = \frac{RT \ln C_s}{C_e} \quad (9)$$

where: q_{mDR} (mg g^{-1}) is the theoretical D–R monolayer capacity, K_{DR} is the D–R constant, C_s is the adsorbate solubility, R is the gas constant, and T is temperature (K).

The commonly misused expression $\varepsilon = RT \ln(1 + 1/C_e)$ is incorrect because the terms 1 and $1/C_e$ are not dimensionally compatible; thus, the definition above is used.

The mean free adsorption energy (E) is calculated from:

$$E = \frac{1}{\sqrt{2K_{DR}}} \quad (10)$$

Values of E: E<8 kJ/mol: physisorption, 8–16 kJ/mol: ion-exchange processes, and >16 kJ/mol: chemisorption

A critical evaluation of adsorption isotherms is essential for understanding how different classes of functionalised adsorbents interact with PMs and Cr(VI) under equilibrium conditions. While the Langmuir, Freundlich, Sips, Temkin, and D–R models provide distinct theoretical frameworks describing monolayer versus multilayer adsorption, surface homogeneity versus heterogeneity, and physical versus chemical adsorption, their real significance emerges when they are applied comparatively across studies.

Assessing which models best describe adsorption for particular adsorbent types, agricultural biosorbents, polymer functionalised materials, and engineered nanocomposites shows trends that go beyond single experiments. These relative patterns help explain why certain classes of adsorbents consistently display multilayer heterogeneous behaviour, why others favour monolayer chemisorption, and why inconsistencies arise when comparable systems are described to follow diverse isotherm models. Hence, merging theoretical models with cross-study evaluation provides deeper insight into adsorption mechanisms, selectivity, and the chemical or structural structures that govern isotherm performance across various adsorbent classes.

Across the literature, the isotherm behaviour of functionalised adsorbents demonstrates clear class-dependent trends. For PM adsorption using engineered nanocomposites, such as Fe_3O_4oMWCNTs, Iqbal et al.[36] reported strong agreement with the Langmuir model, with R^2 values close to unity and high monolayer adsorption capacities (57 mg/g Pt(IV); 104 mg/g Au(III); 112 mg/g Pd(II); 106 mg/g Ag(I)), indicating uniform high affinity binding sites characteristic of chemisorption driven monolayer formation. Similar behaviour was observed by Biata et al.[22], where Fe_3O_4/MgAlLDH nanocomposites exhibited almost perfect Langmuir and Sips fits for Au(III) and Ir(IV), with R^2 values of 0.9976–0.9982 (Langmuir) and 0.9952–0.9977 (Sips) and high adsorption capacities of 124 mg/g and 115 mg/g, respectively, confirming the presence of energetically consistent adsorption sites.

In contrast, Mihăilescu et al.[33] (Figure 10 and Table 1) found that Amberlite XAD7 functionalised with Lglutamic acid exhibited the strongest fit with the Sips isotherm (R^2 = 0.9972), outperforming Langmuir (R^2 = 0.9557) and Freundlich (R^2 = 0.8004). Moreover, the experimentally determined adsorption capacity of 14.23 mg/g closely matched the Sips predicted capacity (14.9 mg/g), while the Sips exponent ($1/n_s$ = −0.71) confirmed the heterogeneous nature of the surface. These results collectively demonstrate that polymer-based and biomolecule-modified resins do not exhibit the same degree of surface uniformity as metaloxide nanocomposites, resulting in isotherm behaviour that incorporates both homogeneous and heterogeneous features better captured by the Sips model.

Table 1. Au(III) onto functionalised Amberlite XAD7 with glutamic acid adsorption isotherm parameters (reproduced from Mihăilescu et al. 2019[33] with permission).

Parameters XAD7-glutamic acid		
Isotherm models	**$q_{m,exp}$ (mgg^{-1}) 14.23**	**Experimental values**
Langmuir	q_L (mgg^{-1})	17.6
	K_L (Lmg^{-1})	0.17
	R^2	0.9557
Freundlich	K_F (mgg^{-1})	3.75
	$1/n_F$	0.39
	R^2	0.8004
Sips	q_s (mgg^{-1})	**14.9**
	K_s	0.32
	$1/n_s$	-0.71
	R^2	**0.9972**

For chromium(VI) and other heavy metals, functionalisation level and adsorbent class play an even more decisive role. In a study by Egbosiuba et al.,[18] MWCNTs decorated with KIAgNPs consistently followed the Langmuir isotherm for Cr(VI), Ni(II), Fe(II), and Cd(II), with R^2 values between 0.962 and 0.971 and low χ^2 values, indicating monolayer adsorption driven by well-distributed active sites created during oxidative and nanoparticle modification. Similar trends were reported by Ihsanullah et al.[31] for modified CNTs and AC with R^2 > 0.9. However, agricultural wastes such as banana waste, Phragmites australis, sawdust, and sugarcane bagasse in a study by El-Baz et al.[38] exhibited model switching: Freundlich behaviour dominated at low concentrations (reflecting surface heterogeneity), whereas Langmuir or Temkin models became more suitable at higher Cr(VI) concentrations. Likewise, studies using magnetitecoated eggshells by Ravi and Sundararaman,[41] phosphoricacidactivated Acacia nilotica by Thilagavathy and Santhi,[42] and modified cherry stones by Gheju et al.[43]consistently followed the Freundlich model ($R^2 \approx 0.97$), confirming multilayer adsorption on highly heterogeneous biomaterial surfaces. These assessments show that synthetic functionalised materials and engineered nanocomposites favour Sips or Langmuir behaviour due to strong chemisorption and structural uniformity, whilst biosorbents, with their fundamentally irregular and various surface chemistries, tend toward Freundlich or, in some circumstances, Temkin behaviour.

Kinetics of adsorption

To interpret the mechanisms governing the relationship between functionalised adsorbents, Cr(VI), and PMs, understanding adsorption kinetics is crucial. Kinetic models are useful for differentiation between chemical and physical adsorption processes, the identification of ratelimiting steps, and the quantification of adsorption rates.[38,41] To be exact, the intraparticle diffusion model offers insight into masstransfer limitations in porous materials. The pseudo–secondorder (PSO) models and pseudo–firstorder (PFO) are extensively employed due to their ability to describe various adsorption systems. When interpreted together, these models provide a thorough understanding of how surface functionalisation, solution conditions, and pore structure determine adsorption performance among various adsorbent classes.

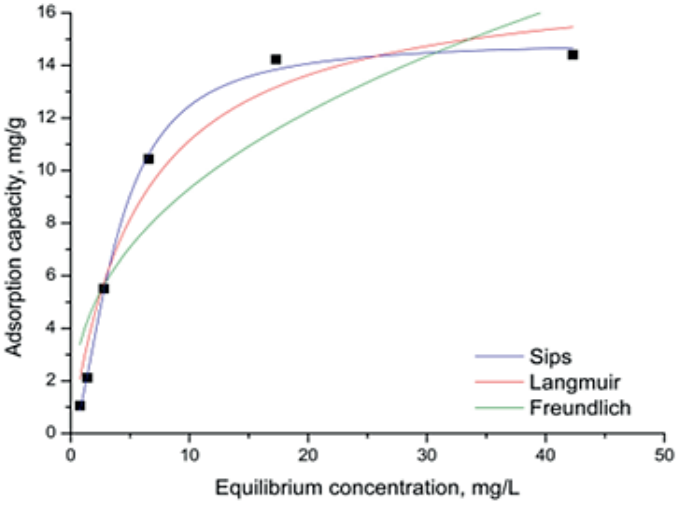


Figure 10. Adsorption isotherms of gold(III) (reproduced from Mihăilescu et al. 2019[33] with permission).

Pseudo–first-order kinetics

The PFO model assumes that the number of available adsorption sites is proportional to the adsorption rate.[38] Equation 11 and 12 represents the linear form of this model, which relates the first-order rate constant (k), the equilibrium adsorption capacity (q_e), and the adsorption capacity at time t (q_t), allowing these variables to be determined from the intercept and the slope of a plot of $\log(q_e - q_t)$ against time:

$$\log(q_e - q_t) = \log q_e - \frac{kt}{2.303} \quad (11)$$

or

$$\ln(q_e - q_t) = \ln q_e - kt \quad (12)$$

The PFO model is often limited to the initial stages of adsorption, whilst it accurately describes systems dominated by external surface interactions, and may underestimate q_e for systems in which diffusion or chemisorption processes dominate.

Pseudo–second-order kinetics

This model is often more appropriate for functionalised adsorbents, particularly when adsorption involves valence forces via electron exchange or sharing.[38] Equation 13 represents the linear expression of the PSO model, which relates time to t/qt, from which both the rate constant (k_2) and equilibrium adsorption capacity (qe) can be determined.

$$\frac{t}{q_t} = \frac{1}{k_2 q_e^2} + \frac{t}{q_t} \quad (13)$$

In comparison to the PFO model, the PSO formulation frequently reveals that chemisorption is the ratecontrolling step and consistently defines adsorption across the full kinetic range, an observation consistent with systems such as chemically modified materials and magnetic nanocomposites exhibiting strong affinity for Cr(VI) and PMs.

Intraparticle diffusion model

To further measure whether diffusion monitors the adsorption rate, this model is applied.[41] Equation 14, the Weber–Morris equation, represents the adsorption capacity at time t (Qt) as a function of the square root of time, including the intercept (C) and intraparticle diffusion constant (K_{id}).

$$Q_t = K_{id} t^{1/2} + C \quad (14)$$

The intercept indicates the thickness of the boundary layer, whereas the K_{id} value reflects the rate of adsorbate molecules into the pores of the adsorbent. If a plot does not pass through the origin, it suggests that the sole ratelimiting step is not intraparticle diffusion and that surface adsorption or external film diffusion also affect the overall kinetics. This model is therefore especially useful in differentiating multistage adsorption mechanisms in porous and hierarchical materials such as activated carbons, CNT-based composites, and LDH-modified nanostructures.

A coherent understanding of adsorption kinetics is essential for interpreting how different functionalised adsorbents interact with PMs and Cr(VI) for determining whether sorption is governed by surface reactions, film diffusion, or intraparticle diffusion. Whereas the PFO and PSO models quantify the rate at which equilibrium is achieved, and the nature of the ratecontrolling step, comparative evaluation across studies reveals broader mechanistic trends that correlate strongly with adsorbent class, surface chemistry, and metalion speciation. This section, therefore, synthesises kinetic behaviours reported in the literature to identify which materials demonstrate chemisorptiondominant adsorption, which exhibit mixed kinetic control, and which factors explain the variability observed between different studies and adsorbent systems.

Mihăilescu et al.[33] recovered Au(III) using Amberlite XAD7 functionalised with Lglutamic acid as shown in Figure 11 and Table 2 and showed that although both PFO and PSO models fitted the data reasonably well ($R^2 > 0.93$), the PSO model gave a markedly superior fit, as evidenced by closer agreement between the predicted

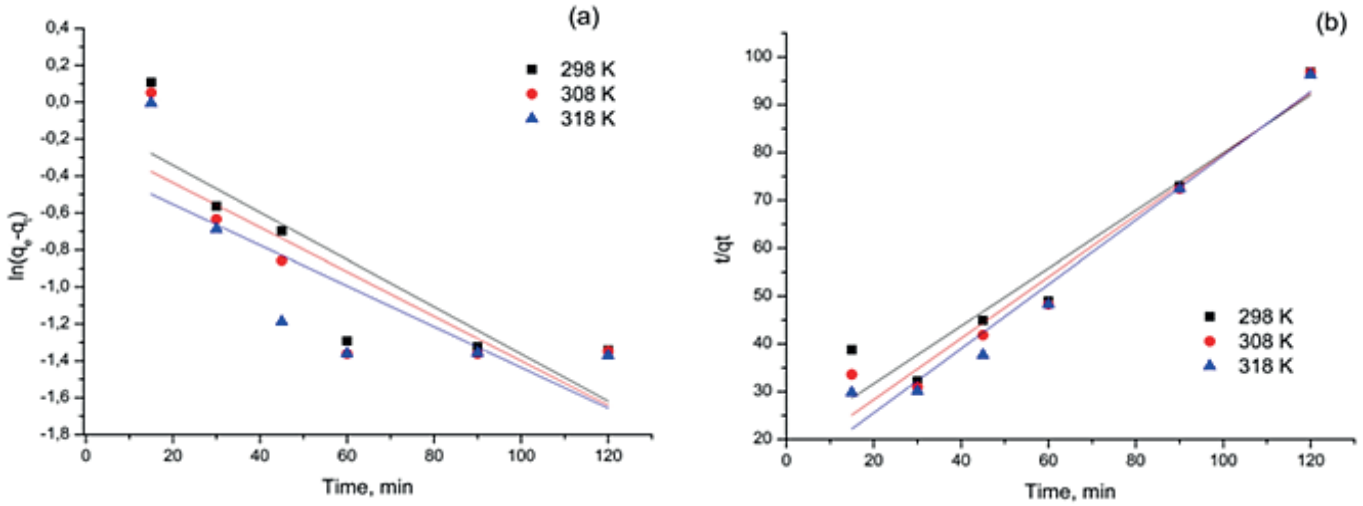


Figure 11. The kinetic mechanism controlling Au(III) adsorption process onto Amberlite XAD7-glutamic acid: (a) PFO; (b) PSO (reproduced from Mihăilescu et al. 2019[33] with permission).

Table 2. Comparison of PFO and PSO rate constants and experimental q_e (reproduced from Mihăilescu et al. 2019[33] with permission).

Temperature (K)	Pseudo-first-order kinetics				Pseudo-second-order kinetics			
	q_e (exp) (mgg^{-1})	k_1 (min^{-1})	q_e (calc) (mgg^{-1})	R^2	q_e (exp) (mgg^{-1})	k_2 (g/mg·min)	q_e (calc) (mgg^{-1})	R^2
298	14.23	0.0047	5.45	0.7626	14.23	36.74	11.82	0.9309
308	14.24	0.0061	5.28	0.7125	14.24	41.93	12.25	0.9561
318	14.25	0.0069	5.25	0.6372	14.25	47.46	12.25	0.968

and experimental qe values (11.82 mg/g predicted vs. 14.23 mg/g experimental at 298 K). Table 2 further shows that the PFO model consistently underestimated q_e (5.25–5.45 mg/g across 298–318 K), whereas the PSO model provided q_e values (11.82–12.25 mg/g) that more closely followed experimental values, demonstrating better predictive power. Additionally, activation energy (E_a = 10.08 kJ/mol) exceeded the theoretical threshold for pure physisorption (4.2 kJ/mol), indicating a physicalchemical adsorption mechanism but with a pronounced chemisorptive component. The authors therefore concluded that the PSO model best captures the ratelimiting interactions between Au(III) and the aminerich functional surface of the modified resin.

Similar mechanistic behaviour was reported by Grad et al.[37] using ChitosanDB18C6 for the recovery of Ru(III), Pd(II), and Pt(IV), where both high R^2 values (>0.99) and high activation energies (E_a > 40 kJ/mol) confirmed chemisorption as the dominant mechanism. The consistency between these two studies, despite different adsorbent matrices, indicates that polymer-based adsorbents functionalised with donor groups such as amines, amides, or crown ethers generally favour chemisorption-controlled kinetics, reflected in strong PSO behaviour. This suggests that ligand metal coordination, rather than physical attraction or diffusion, primarily governs adsorption rates for such materials.

A similar trend was observed for nanocomposite-based adsorbents. Egbosiuba et al.,[18] evaluated the kinetics of Cd(II), Ni(II), Fe(II), and Cr(VI) adsorption onto MWCNTs decorated with silver nanoparticles synthesised via green chemistry. Within the first 60 minutes, a rapid initial uptake occurred, associated with the strong electrostatic, π electron interactions and abundance of vacant active sites. Adsorption reduced and reached equilibrium when active sites became saturated. For all metal ions tested, PSO exhibited lower error statistics and higher R^2 values compared to PFO, emphasising that strong surface interactions or chemisorption dominate the adsorption mechanism for CNTbased nanocomposites. Similar results were obtained by El-Baz et al.[38] utilising agricultural residual adsorbents for Cr(VI), where PSO also exhibited the best fit, implying that even biosorbents can display chemisorptionlike behaviour when metalion binding involves specific functional groups such as lignocellulosic, phenolic, or carboxyl.

Ihsanullah et al.[31] further supported the dominance of the PSO model across various classes of adsorbents. The study reported R^2 values exceeding 0.99 for both modified CNTs and AC in the adsorption of Cr(VI). These data indicate that enhancements in carbon surface chemistry, particularly enhanced oxygen-containing functional groups after acid oxidation, increase specific interactions with Cr(VI), resulting in PSO kinetics for this adsorption. Similarly, Fe_3O_4 carbon nanocomposite produced from agricultural waste demonstrated that PSO (R^2 = 0.9962) surpassed PFO (R^2 = 0.9426), as reported by Mohamed Khalith et al.,[35] verifying that the introduction of carbon and iron oxides improves chemisorption properties. Sherlala et al.[44] in a review of organofunctionalised magnetic graphene oxide (OFMGO) nanocomposites, also concluded that PSO is the predominant model describing heavy metals adsorption for these materials, showing that chemisorptive interactions are typical across advanced carbon-based and magnetic composites.

A broader synthesis of these outcomes establishes various main mechanistic patterns. First, adsorbents from agricultural residues, regardless of their heterogeneity, often exhibit PSO behaviour when Cr(VI) is involved since it undergoes complexation and reduction reactions during adsorption, processes fundamentally related to chemisorption. Second, functionalised nanocomposites such as Fe_3O_4containing materials, graphenebased, and CNTbased, consistently display PSOdominated kinetics due to their highaffinity active sites and high uniform density, which promote surface complexation and electron transfer. Lastly, biopolymerbased and polymeric materials, including ChitosanDB18C6 and Amberlite XAD7–glutamic acid, also exhibit strong chemisorptive behaviour, reflected in higher activation energies and elevated R^2 values in PSO.

Notably, the few instances where PFO or mixedorder behaviour appear in the literature generally correspond to systems dominated by rapid surface sorption or weak physical interactions rather than surface functionalisation. Hence, the occasional inconsistencies across studies arise not from procedural irregularities but from fundamental differences in pore structure, the presence or absence of specific functional groups, and surface chemistry capable of forming chemical bonds with metal ions.

Overall, the comparative analysis clearly shows that PSO is the dominant kinetic model for functionalised adsorbents used in the recovery of PMs and the removal of Cr(VI), reflecting the prevalence of chemisorption and strong adsorbent metal interactions across these systems. Differences in kinetic behaviour between materials can thus be explained by the nature of their active sites, the degree of functionalisation, and the inherent reactivity of the target metal ions.

Adsorption thermodynamics

Adsorption thermodynamics provide essential insight into the feasibility, spontaneity, and energetic nature of metalion uptake by functionalised adsorbents.[39] A comparative assessment reveals mechanistic patterns that distinguish adsorbent classes and explain why certain materials exhibit superior performance for Cr(VI) removal or PM recovery, rather than explaining isolated values of ΔS°, ΔH°, and ΔG° from specific papers. The principal equilibrium variables relating temperature to adsorption are obtained from the expression (Equation 15):[18]

$$\Delta G^{o} = -RT\ln K \quad (15)$$

where R is the gas constant, T is the temperature (K), and K is the equilibrium constant. Figure 12 illustrates the Van't Hoff relation, derived from Equation (15), which enables simultaneous determination of d ΔS° and ΔH° from the intercept and slope of ln K versus 1/T.

$$\Delta G^{o} = \Delta H^{\circ} - T\Delta S^{\circ} \quad (16)$$

Together, these parameters indicate whether adsorption is chemisorptive, physisorptive, entropydriven, and enthalpydriven, allowing meaningful interpretation of adsorption mechanisms and selectivity across adsorbent classes.

Au(III) adsorption onto Amberlite XAD7 modified with Lglutamic acid demonstrated thermodynamic behaviour which are broadly consistent with patterns commonly observed for ligandfunctionalised polymer resins as reported by Mihăilescu et al.[33] (Table 3). As exhibited in Figure 12 & Table 3, the process displayed a positive entropy change (ΔS° = 55.8 J/mol·K), moderately negative Gibbs free energy values (ΔG° ranging from −1.22 to −2.33 kJ/mol across 298–318 K) and a moderately positive enthalpy change (ΔH° = 15.43 kJ/mol). The positive ΔS° likely indicates increased interfacial disorder, potentially linked to configurational rearrangements within the resin and partial dehydration of Au(III) species during ligand exchange. The increasingly negative ΔG° values indicate that spontaneity may increase slightly with temperature, whilst the positive ΔH° suggests that adsorption is endothermic under the studied conditions. Figure 12 exhibits the linearity of the van't Hoff plot, which further supports temperature-dependent favourability, a behaviour frequently interpreted as consistent with endothermic chemisorption involving metal–ligand coordination, although contributions from polymermatrix relaxation or hydrationshell disruption cannot be excluded.

Similar thermodynamic behaviour has been reported for other polymermodified adsorbents. For instance, Grad et al.[37] reported positive ΔS° values often exceeding 80 J/mol·K, corrected from the original kJ/mol·K units, ΔH° values ranging from 21.34 to 43.3 kJ/mol, and negative ΔG° values between −2.84 and −7.07 kJ/mol for the ChitosanDB18C6 system examined. These together support an endothermic chemisorption mechanism, entropyenhanced, even though the comparative contributions of polymeric conformational

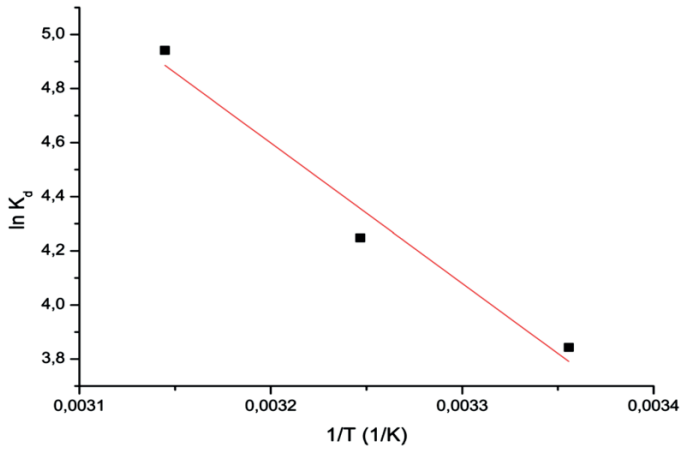


Figure 12. The adsorption of Au(III) onto Amberlite XAD7-glutamic acid Van't Hoff plots (reproduced from Mihăilescu et al. 2019[33] with permission).

Table 3. Thermodynamic parameters for the adsorption of Au(III) onto Amberlite XAD7-glutamic acid with (reproduced from Mihăilescu et al. 2019[33] with permission).

Temperature (K)	ΔH° (kJmol^{-1})	ΔS° (J/mol·K)	ΔG° (kJmol^{-1})	R^2
298	15.43	55.8	-1.22	0.9718
308			-1.77	
318			-2.33	

adjustment, dehydration, and ion pairing may vary across systems. Together, these results suggest that PM adsorption onto LDH-modified and polymeric adsorbents often, although not collectively, exhibits thermodynamic signatures indicative of entropydriven and moderate enthalpy chemisorption.

Conversely, Cr(VI) adsorption exhibits a broader range of thermodynamic behaviours, indicating the impact of chromium speciation (CrO_4^{2-} versus $HCrO_4^-$), difference in surface heterogeneity, and variations in redox activity across adsorbents. Small positive ΔS° and slightly exothermic behaviour (ΔH° ≈ −0.0787 kJ/mol) were reported by Ume et al.[39] using *Aspergillus niger*, a pattern consistent with primarily outersphere, substantially driven interactions in systems where electrontransfer pathways are restricted. Most agricultural and related materials exhibit correspondingly minimal enthalpy changes unless chemically modified, implying weaker sorption forces and restricted specificity in their natural form. Further variations appear when Egbosiuba et al.,[18] reported ΔG° values that remained negative across temperatures, confirming spontaneity but indicating lowenthalpy and entropy-dominated adsorption. Furthermore, the ΔH° values with units corrected from kJ/mol to J/mol: 706.70–2153.33 J/mol which clearly fall within the physisorption domain, below the >40 kJ/mol threshold naturally associated with chemisorption. Lastly, even though ΔS° values remain positive (118.61–124.34 J/mol·K), implying interfacial disorder, these magnitudes are better explained as suggesting nonspecific entropy gains rather than strong coordination. Likewise, Mohamed Khalith et al.,[35] reported the endothermic behaviour for Fe_3O_4–carbon nanocomposites produced from agrowaste seems consistent with lowtomoderate enthalpy adsorption, also established within the physisorption range.

Overall, performance differences across adsorbent classes could be explained by these distinct thermodynamic signatures. PM adsorption onto LDH hybrids and polymerfunctionalised resins classically displays moderately negative ΔG°, strongly positive ΔS°, and moderately positive ΔH° behaviour consistent with relatively weak chemisorption and ligandmediated interactions. Cr(VI) adsorption, nevertheless, exhibits greater inconsistency depending on whether reduction to Cr(III) happens during uptake: redoxactive adsorbents frequently display larger (yet still modest) entropy and enthalpy changes, whilst systems relying largely on electrostatic interactions exhibit significantly reduced values. Evident inconsistencies between available thermodynamic datasets are hence more reasonably attributable to variations in redox activity, Cr(VI) speciation, and surface chemistry than to operational limitations. Egbosiuba et al.,[25] provided thermodynamic evidence when reported with suitable unit correction, that reflects entropydriven physisorption, lowenthalpy; more generally, these variables remain valuable indicators of adsorption energetics and help distinguish whether Cr(VI) or PMs removal or recovery proceeds through redoxactive pathways, electrostatic interactions, or ligandmediated coordination.

SCALE-UP CONSIDERATIONS AND PRACTICAL APPLICATION

Even though adsorption is broadly defined as environmentally favourable and a costeffective strategy, its adaptation to industrial practice, starting with laboratory studies, may require thorough evaluation. Bilal et al.,[9] reported that, specifically when lowcost precursors such as foodwaste biomass and agricultural residues are used, adsorption can be economically beneficial, reducing reliance on increasingly costly commercial AC. Studies by Amuanyena et al.,[20] Zhu et et al.,[30] and Bediako et al.,[25] further reported that biomassderived materials incorporating Moringa seed proteins, pomegranate peel, and orange peel may serve as inexpensive, abundant, and renewable substitutes that offer high adsorption possibilities for Cr(VI) and PMs. Furthermore, the economic argument for adsorption has been highlighted by Aghaei et al.,[2] and Reith et al.[1] emphasising that extracting PMs such as Pd, Pt, Ir, and Au through adsorption may support both resource circularity and environmental protection.

From an operational assessment, studies such as those by Alshammari et al.,[10] Bilal et al.,[9] and Krishnan et al.,[8] suggest that adsorption procedures may be more environmentally friendly and require less sophisticated infrastructure than ion flotation, chemical precipitation, and membrane filtration, all of which can generate secondary waste and excessive reagent use. All these support that adsorption is typically regarded as environmentally friendly and economical. Additionally, the sustainability of adsorption may be strengthened by utilising green solvents: Abdullah and Kadhom[45] and Lanaridi et al.[46] have investigated deep eutectic solvents (DESs) as energyefficient media, biodegradable, and nontoxic, which suggests additional prospects for greener largescale use.

The possibility of scaleup is also associated with adsorbent durability and regeneration. For instance, Egbosiuba et al.[18] reported that MWCNTs–KIAgNPs could be recycled for up to eight adsorption–desorption cycles while maintaining over 80% metalion removal efficiency, suggesting favorable operational longevity if such behaviour is sustained under an industrial environment. Grad et al.[37] reported similar multicycle performance for ChitosanDB18C6 material, which may imply that several functionalised adsorbents could strengthen longterm cyclic application in continuous treatment approaches.

Regardless of these reassuring results, various authors caution that scaleup may present operational setbacks. For example, Mourdikoudis et al.[23] and Anyika et al.[16] report that carbonbased nanomaterials can aggregate in solution, theoretically reducing efficiency in largevolume reactors, although functionalisation approaches may alleviate this tendency. Multiple studies, including those by Ihsanullah et al.[31] Egbosiuba et al.,[18] Grad et al.[37] and Mihăilescu et et al.,[33] further show that adsorption performance is highly pH-dependent, suggesting that industrial wastewaters with varying acidity may require preconditioning to maintain efficiency. In addition, equilibrium times reported by Ihsanullah et al.[31] Iqbal et al.,[34] and Mihăilescu et al.,[33] change widely across materials from quick uptake within minutes to several hours, suggesting that flow dynamics, residence time, and reactor design may need casespecific optimisation during scaleup. Spectroscopic and thermogravimetric analyses reported by Ihsanullah et al.[31] Padmavathy et al.,[19] and Amuanyena et al.,[20] further imply

that the chemical and thermal stability of adsorbents may impact their longterm performance under industrial environments and consequently should be integrated into the method model.

Together, while the literature reviewed commonly supports the possibility of functionalised adsorbents as environmentally favourable, costeffective, and regenerable materials, authors across several studies emphasise that their effective industrial application may depend on addressing aggregation behaviour, stability, contacttime optimization, and pH sensitivity under realistic wastewater conditions. These reflections may inform upcoming research and assist in bridging the gap between largescale deployment, practical, and laboratory demonstrations.

RECOVERY AND RECYCLING

Recovery or removal of precious metals (PMs) and Cr(VI) from spent functionalised adsorbents is essential for ensuring the environmental sustainability, economic viability, and circulareconomy relevance of adsorption technologies. A variety of recovery techniques have been reported, including traditional chemical desorption using mineral acids, thermal decomposition of spent adsorbents, and solventbased extraction systems such as emerging deep eutectic solvents (DESs). These approaches share the common objective of selectively isolating metal ions for reuse or further processing, while enabling the regeneration of adsorbents so that multiple adsorption–desorption cycles can be achieved.

Traditional regeneration methods rely primarily on mineral acid desorption, in which protonation weakens metal ligand interactions at the adsorbent surface. For example, Biata et al.[22] regenerated Fe_3O_4/Mg–Al–LDH nanocomposites loaded with Au(III) and Ir(IV) using 3 M H_2SO_4, followed by magnetic separation and washing with ethanol and deionised water before drying. Similarly, Egbosiuba et al. [18] regenerated MWCNTs decorated with Ag nanoparticles by shaking the spent adsorbent with 0.5 M H_2SO_4 at 40 °C, yielding successful multimetal desorption and allowing up to eight reusability cycles with metalion removal efficiencies exceeding 80%. Chemical desorption is thus effective where adsorption is dominated by electrostatic attraction or ion exchange; however, acid consumption and potential adsorbent degradation highlight the need for greener alternatives.

A second category comprises thermal decomposition techniques, which are particularly suited for polymeric or biomaterialbased adsorbents that form strong innersphere complexes with precious metals. Mihăilescu et al.[33] demonstrated this by thermally decomposing Amberlite XAD7 modified with Lglutamic acid after Au(III) adsorption (Table 3). Thermogravimetric analysis was used to identify the necessary temperature ranges, and the samples were subsequently heated up to 1 273 K to yield metallic gold, which was confirmed by SEM–EDX. Thermal decomposition was also successfully applied by Grad et al.[37] to recover Pt(IV), Pd(II), and Ru(III)from spent ChitosanDB18C6 adsorbents. Although effective for highvalue PM recovery, thermal routes can be energy-intensive, making them more suitable for PM streams where high-purity yields justify energy costs.

Solvent-based regeneration represents a third category, where conventional organic solvents or emerging green solvents are used to dissolve or disrupt adsorbate surface interactions. Within solventbased strategies, deep eutectic solvents (DESs) have emerged as a more sustainable and increasingly preferred alternative. DESs are formed by combining a hydrogenbond donor (HBD) with a hydrogenbond acceptor (HBA), producing a eutectic mixture with a significantly depressed melting point relative to the starting components. As described by Abdullah and Kadhom,[45] a mixture of choline chloride and urea (2:1) decreases in melting point from 302 °C to 133 °C to only 12 °C due to the extensive hydrogenbonding network in the DES. These solvents offer low toxicity, low vapour pressure, high thermal stability, and water tolerance, making them attractive substitutes for conventional organic solvents.

DESs have proven particularly effective for recovering platinumgroup metals (PGMs). Lanaridi,[46] applied cholinebased DESs to extract these PGMs from spent automotive catalysts under energy-efficient conditions. The mechanism is attributed to the strong coordination ability of DES components, which stabilise metalchloro complexes through hydrogen bonding and donor–acceptor interactions, enhancing metal solubilisation. Likewise, Yuan et al[47] reported ethaline (ethylene glycol: choline chloride) as an efficient DES for recovering gold, palladium, and silver from industrial effluent, also enabling the regeneration of adsorbents previously used to remove Pb(II), Zn(II), and Fe(III). Tunability of DES composition allows solvation strength, viscosity, and metalligand interactions to be optimised for specific target ions.

Generally, these recovery pathways emphasise the importance of regeneration in enabling a circulareconomy methodology to functionalised adsorbents. Thermal decomposition offers highpurity metal recovery, but at a superior energy cost. Traditional mineralacid desorption remains efficient but can generate chemical waste and decrease adsorbent longevity. Conversely, DESs offer reduced environmental burden, tunability, and high efficiency, providing a favorable path for sustainable adsorbent recycling and PM recovery.

VARIOUS FUNCTIONALISED ADSORBENTS COMPARATIVE PERFORMANCE

The improved performance of functionalised adsorbents compared to conventional materials has been consistently demonstrated across studies exploring the recovery and removal of Cr(VI) and PMs. Their strong selectivity, high adsorption capacity, and superior stability arise from the careful integration of functional groups that promote specific metal ligand interactions, together with naturally well-developed porosity and large surface areas. These chemical and structural features facilitate improved recyclability, faster kinetics, and more efficient binding compared with unmodified adsorbents. Table 4 provides a consolidated overview of adsorbent characteristics and adsorption variables to demonstrate these comparative advantages reported in several independent investigations.

A holistic evaluation of the parameters in Table 4 shows that the performance of functionalised adsorbents is strongly dependent on the interplay between pH, equilibrium time, surface area, isotherm behaviour, kinetic control, and regeneration capacity, with clear mechanistic differences between PM recovery and Cr(VI) removal. For PM systems, the strongest adsorption is achieved under highly acidic conditions (typically pH ≤ 4), which favour the formation of stable PMchloro complexes and enhance interaction with protonated functional groups. This trend is most pronounced for the H_2SO_4activated biomassderived carbon reported by Bediako et al.,[25] which achieved a remarkable Au(III) adsorption capacity of 1680 mg/g, the highest in Table 4 under strongly acidic conditions, reflecting the synergistic effect of extensive microporosity and dense acidic surface functionalities.

Polymermodified adsorbents such as Amberlite XAD7–glutamic acid Mihăilescu et al.[33] and ChitosanDB18C6 Grad et al.[37] exhibit lower adsorption capacities (14.23–30.4 mg/g) but rely on specific ligand–metal coordination, as confirmed by their excellent fits to Langmuir and Sips isotherm models, indicating monolayer chemisorptive binding. The Fe_3O_4/Mg–AlLDH hybrid Biata et al.[22] reaches higher capacities (115–124 mg/g for Ir(IV) and Au(III)) due to the presence of anionexchange layers and metaloxide sites, which enhance innersphere complexation at low pH.

Effects of temperature also vary greatly across PM systems: Several PM adsorbents function successfully at 25 °C, including Amberlite XAD7–glutamic acid and Fe_3O_4/Mg–AlLDH, suggesting that high PM uptake does not require high temperatures. Conversely, ChitosanDB18C6 exhibits slightly improved recovery at 45 °C, demonstrating moderate thermal stimulation of ligand mobility. PM targeting adsorbents also

Table 4. Comparison of the adsorbent properties and adsorption parameters across several studies.

Adsorbate	Adsorbent	Time (min)	pH	Temp (˚C)	Isotherm/ kinetics models used	Cycles	Surface area (m^2/g)	q_m (mg/g)	Reference
Au(III)	Fe_3O_4/Mg-Al-LDH)	27	4.5	25		10	134.2	124	Biata et al.[22]
Ir(IV)	Fe_3O_4/Mg-Al-LDH	27	4.5	25	Sips/PSO & Langmuir	10	134.2	115	Biata et al.[22]
Au(III)	Amberlite XAD7 resin/L-glutamic acid	60	<4.0	25		*	*	14.23	Mihăilescu et al.[33]
Pt(IV)	Chitosan-DB18C6	180	<3	45		5	14.44	17.6	Grad et al.[37]
Pd(II)	Chitosan-DB18C6	180	<3	45	Sips/PSO	3	14.44	22.6	Grad et al.[37]
Ru(III)	Chitosan-DB18C6	180	<3	45		5	14.44	30.4	Grad et al.[37]
Pd(II)	Fe_3O_4-o-MWCNTs	180	2	25		5	*	112	Iqbal et al.[34]
Pt(IV)	Fe_3O_4-o-MWCNTs	180	2	25		5	*	57	Iqbal et al.[34]
Ag(I)	Fe_3O_4-o-MWCNTs	180	2	25	Langmuir/ PSO	5	*	106	Iqbal et al.[34]
Au(III)	Fe_3O_4-o-MWCNTs	180	2	25		5	*	104	Iqbal et al.[34]
Pd(II)	PPy-CS_2@SiO_2@ Fe_3O_4	15	6	20		5	38.0	163.0	Poudel et al.[48]
Au(III)	PPy-CS_2@SiO_2@ Fe_3O_4	15	6	20		5	38.0	132.7	Poudel et al.[48]
Pt(IV)	Modified pomegranate peel	3 000	1	25		*	*	1.16	Zhu et al.[30]
Pd(II)	Modified pomegranate peel	3 000	1	25		*	*	1.05	Zhu et al.[30]
Au(III)	Modified pomegranate peel	30	1	25		*	*	34.0	Zhu et al. [30]
Pt(IV)	HI-MC	120	4-5	25		5	10.4	105	Hashem et al.[49]
Pd(II)	HI-MC	120	4-5	25	Langmuir/ PSO	5	10.4	88	Hashem et al.[49]
Au(III)	HI-MC	120	4-5	25		5	10.4	75	Hashem et al. [49]
Au(III)	Au Biomass-derived AC H_2SO_4	180	1	25		4	1211.22	1680	Bediako et al.[25]
Cr(VI)	MWCNTs-KIAgNPs	60	3	60		5	1236± 5.40	229.540±0.001	Egbosiuba et al.[18]
Ni(II)	MWCNTs-KIAgNPs	60	6	60		5	1236± 5.40	174.784±0.006	Egbosiuba et al.[18]
Fe(II)	MWCNTs-KIAgNPs	60	6	60		5	1236± 5.40	149.552±0.005	Egbosiuba et al.[18]
Cd(II)	MWCNTs-KIAgNPs	60	6	60		5	1236± 5.40	121.026±0.003	Egbosiuba et al.[18]
Cr(VI)	Acid-modified CNTs	120	4	*		*	170	1.314	Ihsanullah et al.[31]
Cr(VI)	Acid-modified AC	240	3	*	Langmuir/ PSO	*	1 420	18.519	Ihsanullah et al.[31]

Footnote: Where entries are marked "no data/not studied," the respective studies did not report measurements for those parameters and therefore could not be included in the comparative evaluation.

differ in equilibrium times: Polymeric systems require 60–180 min, whereas Fe_3O_4/Mg–AlLDH approaches equilibrium quickly at 27 min, suggesting slower intraparticle diffusion through compact matrices.

Kinetic investigation of the studied PM materials by Biata et al.,[22] Grad et al.,[37] and Mihăilescu et al.[33] constantly supports PSO models, implying chemisorption-controlled uptake. Reusability is strongest for LDHbased systems: Fe_3O_4/Mg–AlLDH maintains high efficiency over 10 cycles, whereas polymerbased adsorbents retain performance over 3–5 cycles, indicating stable but more limited regeneration behaviour.

In contrast, Cr(VI) removal presents a different pattern because Cr(VI) exists in multiple oxyanion forms ($HCrO_4^-$, CrO_4^{2-}), and adsorption depends heavily on surface charge and, where present, redox capability. The MWCNTs–KIAgNPs composite Egbosiuba et al.[25] shows the highest Cr(VI) capacity in the table (229.54 mg/g) at pH 3, where monovalent $HCrO_4^-$ dominates and strong electrostatic attraction occurs between the anion and the positively charged nanotube surface. Equilibrium is achieved within 60 min, and adsorption follows the Langmuir isotherm and PSO kinetics, indicating monolayer chemisorption like behaviour despite the overall physisorptive energetics reported in the literature for similar systems.

By contrast, the acidmodified CNTs and activated carbon reported by Ihsanullah et al.[31] exhibit substantially lower Cr(VI) adsorption capacities (1.314 and 18.519 mg/g, respectively) and require much longer equilibrium times (120–240 min). Their adsorption performance is governed mainly by surface acidity and electrostatic attraction rather than redox transformation, accounting for their comparatively weak removal efficiency. Temperature effects were not reported for these systems, which limits direct comparison with thermally responsive adsorbents. In the study by Egbosiuba et al.,[18] the Cr(VI) adsorbent based on MWCNTs–KIAgNPs maintained acceptable performance over five regeneration cycles, although the gradual decline in efficiency suggests susceptibility to oxidative structural degradation.

Taken together, the data in Table 4 indicate that high PM recovery is achieved when several parameters converge: strongly acidic pH, high surface area, the presence of ligandspecific coordination sites, favourable monolayer adsorption (typically Langmuir behaviour), PSOtype chemisorption kinetics, and stable regeneration performance. In contrast, successful Cr(VI) removal relies more on acidic operating conditions, favourable surface charge, moderate temperatures, and rapid

electrostatic or redoxassisted interactions. These numerous systematic limitations explain why Cr(VI) systems exhibit wider variability, whereas PM focusing adsorbents consistently show more predictable capacities and superior performance across the materials evaluated.

CONCLUSION

Functionalised adsorbents continue to exhibit substantial potential as adaptable materials for the removal and recovery of Cr(VI), PMs, and various pollutants from aqueous media. Their adaptable structural properties, tunable surface chemistry, and high surface area enable strong interactions with a wide range of target species, including gold, platinum, palladium, silver, ruthenium, iridium, several organic pollutants, and heavy metals. Even though performance varies across material classes, the ability to modify functional groups such as –COOH, –NH_2, and –SH offers opportunities to enhance adsorption affinity and selectivity, thereby enhancing overall removal efficiency.

A wide range of functionalisation approaches and synthesis, incorporating templateassisted, hydrothermal, sol–gel processing, and chemical vapour deposition procedures, continues to expand the operational range of these adsorbents. Composite and hybrid systems, predominantly those involving metal oxides or polymers, further enhance electrical, magnetic, and mechanical properties, often enabling improved reusability and separation efficiency. Thorough characterisation with zeta potential, FTIR, BET, XRD, TGA, SEM, and VSM analysis provides the chemical and structural understanding required to justify functionalisation and appreciate structure–performance interactions.

Variables, namely initial metalion concentration, temperature, adsorbent dosage, contact time, and pH, influence the adsorption behaviour of functionalised adsorbents. Isotherm and kinetic studies remain fundamental for interpreting modelling equilibrium behaviour and adsorption mechanisms, optimising process environments. Although adsorption often exhibits PSO kinetics and Sips or Langmuir isotherm models, differences across adsorbent categories demonstrate the necessity for systemspecific assessment rather than broad assumptions.

Recovery of PMs from used adsorbents is also a fundamental part of ecological effluent treatment. Several extraction and regeneration approaches involving solvent extraction (gradually utilising greener solvents such as DESs), chemical precipitation, electrodeposition, and membrane-based processes have shown potential for selective recovery of PMs and restoring adsorbent functionality. These methods support circulareconomy objectives by aiding resource recovery and pollutant removal.

Generally, this review offers a combined perspective on recovery pathways, surfacefunctionalisation strategies, operational influences, adsorption mechanisms, and synthesis approaches associated with functionalised adsorbents. Although considerable progress has been made, further research may still be required to enhance regeneration effectiveness, longterm stability, scalability, and performance under realistic effluent conditions. Nevertheless, the collective evidence indicates that functionalised nanomaterialbased adsorbents remain among the most promising candidates for advancing efficient and sustainable remediation technologies for wastewater contaminated with PMs, Cr(VI), and other pollutants.

FUTURE OUTLOOK AND CHALLENGES

The future development of functionalised adsorbents for the recovery or removal of precious metals (PMs) and chromium(VI) may require addressing several fieldrelevant challenges that go beyond the promising laboratory findings reported by Amuanyena et al.,[20] Mihăilescu et al.,[33] Grad et al.,[37] and Egbosiuba et al.[18] Although these studies demonstrate strong adsorption capacities under controlled conditions, mechanistic understanding may still be incomplete, particularly because pHdependent speciation and surfacecharge transitions such as those highlighted by Mihăilescu al.[33] for Au(III) and Egbosiuba al.[18] for Cr(VI) may behave unpredictably in real wastewater environments where competing ions, colloids, and organic compounds coexist. Similarly, although regeneration outcomes are encouraging, with Biata al.[22] showing stable reuse of Fe_3O_4/MgAlLDH nanocomposites and Egbosiuba et al.[18] reporting up to eight effective cycles for MWCNTsKIAgNPs, longterm stability under realistic conditions remains uncertain due to potential pore blockage, functionalgroup degradation, or matrix interference.

Furthermore, most adsorption studies, including those by Grad et al.,[37] Zhu et al.,[30] and have been conducted using synthetic or simplified systems, which may not fully capture the complexity of industrial effluents that contain diverse metal ions, surfactants, and suspended solids. Scaleup could be challenging since largescale reactors should contend with pHsensitivity noted by Grad al.,[37] and Mihăilescu et al.,[33] material aggregation reported by Anyika et al.,[16] and mixing limitations or potential flow. Environmental and economic considerations may also require closer attention; although adsorption has been regarded as costeffective by authors such as Bilal al.,[9] practical implementation will likely depend on ensuring consistent quality of biomass precursors, evaluating the sustainability of synthesis protocols demonstrated by Bediako al.,[25] and Zhu et al.,[30] and assessing the feasibility of greener regenerants such as deep eutectic solvents proposed by Lanaridi al.[46]

To address these issues, future research may benefit from a structured roadmap that includes clarifying surfaceinteraction mechanisms under multiion conditions, validating adsorbent performance in real wastewater matrices, improving regeneration durability, developing scaleappropriate reactor configurations for functionalised adsorbents, and conducting lifecycle and technoeconomic analyses to evaluate environmental sustainability and industrial viability.

SUPPLEMENTARY INFORMATION

There is no supplementary information.

ACKNOWLEDGMENTS

The authors acknowledge support from these universities: Namibia University of Science and Technology (NUST) and University of South Africa (UNISA) in preparation of this paper. The authors have revised and altered the output and take full accountability for the content of this publication.

AUTHOR CONTRIBUTIONS

Conceptualisation, M.A.E.; writing—original draft preparation, M.A.E.; writing—review and editing, H.M.K, M.M.N and D.S. All authors have examined and accepted to the published version of the manuscript.

DECLARATION OF COMPETING OR FINANCIAL INTEREST

No conflict of interest is declared by the authors, and no external funds were used for this research.

DECLARATION OF GENERATIVE AI AND AI-ASSISTED TECHNOLOGIES

Quillbot and Copilot were used to correct the grammar in this article.

AUTHOR ORCIDS

Marta O.N.A. Elvin: https://orcid.org/0009-0002-1001-3940
Mathew M. Nindi: https://orcid.org/0000-0001-7222-1505
Habauka M. Kwaambwa: https://orcid.org/0000-0001-9378-9933
Simi Dube: https://orcid.org/0009-0002-7482-3945

COPYRIGHT PERMISSIONS FOR REPRODUCED FIGURES

The authors confirm that written permission was obtained for all reproduced figures and is available upon request, in accordance with standard journal practice.

REFERENCES

1. Reith F, Campbell SG, Ball AS, Pring A, Southam G. Platinum in Earth surface environments. Earth Sci Rev. 2014;131:1–21. https://doi.org/10.1016/j.earscirev.2014.01.003.
2. Aghaei E, Alorro RD, Encila AN, Yoo K. Magnetic adsorbents for the recovery of precious metals from leach solutions and wastewater. Metals (Basel). 2017;7(12):529. https://doi.org/10.3390/met7120529.
3. Cayumil R, Khanna R, Rajarao R, Mukherjee PS, Sahajwalla V. Concentration of precious metals during their recovery from electronic waste. Waste Manag. 2016;57:121–130. https://doi.org/10.1016/j.wasman.2015.12.004.
4. Sharma S, Krishna Kumar AS, Rajesh N. A perspective on diverse adsorbent materials to recover precious palladium and the way forward. RSC Adv. 2017;7(82):52133–52142. https://doi.org/10.1039/C7RA10153H.
5. Lau YJ, Khan FSA, Mubarak NM, Lau SY, Chua HB, Khalid M, Abdullah EC. Functionalized carbon nanomaterials for wastewater treatment. In: Thomas S, Grohens Y, Pottathara YB (editors), Industrial Applications of Nanomaterials. Amsterdam: Elsevier Inc.; 2019. pp. 283–311. https://doi.org/10.1016/B978-0-12-815749-7.00010-4.
6. Nikoloski AN, Ang KL. Review of the application of ion exchange resins for the recovery of platinum-group metals from hydrochloric acid solutions. Miner Process Extr Metall Rev. 2014;35(6):369–389. https://doi.org/10.1080/08827508.2013.764875.
7. Yahorava V, Kotze M. Ion exchange technology for the efficient recovery of precious metals from waste and low-grade streams. J South Afr Inst Min Metall. 2014;114(2):173–181.
8. Krishnan S, Zulkapli NS, Kamyab H, Taib SM, Din MFBM, Majid ZA, Chaiprapat S, Kenzo I, Ichikawa Y, Nasrullah M, et al. Current technologies for recovery of metals from industrial wastes: an overview. Environ Technol Innov. 2021;22: 101525. https://doi.org/10.1016/j.eti.2021.101525.
9. Bilal M, Shah JA, Ashfaq T, Gardazi SMH, Tahir AA, Pervez A, Haroon H, Mahmood Q. Waste biomass adsorbents for copper removal from industrial wastewater-A review. J Hazard Mater. 2013;263:322–333. https://doi.org/10.1016/j.jhazmat.2013.07.071.
10. Alshammari MS, Derafa W, Elshaygi EAA. Removal of heavy metals from groundwater using silica/activated carbon composite. Desalination Water Treat. 2021;238:198–206. https://doi.org/10.5004/dwt.2021.27774.
11. Tamjidi S, Moghadas BK, Esmaeili H, Shakerian Khoo F, Gholami G, Ghasemi M. Improving the surface properties of adsorbents by surfactants and their role in the removal of toxic metals from wastewater: A review study. Process Saf Environ Prot. 2021;148:775–795. https://doi.org/10.1016/j.psep.2021.02.003.
12. Alshammari MS, Derafa W, Elshaygi EAA. Removal of heavy metals from groundwater using silica/activated carbon composite. Desalination Water Treat. 2021;238:198–206. https://doi.org/10.5004/dwt.2021.27774.
13. Krishna D, Sree RP. Artificial Neural Network and Response Surface Methodology Approach for Modeling and Optimization of Chromium (VI) Adsorption from Waste Water using Ragi Husk Powder. Indian Chem. Eng. 2013;55(3):200–222. https://doi.org/10.1080/00194506.2013.829257.
14. Demiral İ, Samdan C, Demiral H. Enrichment of the surface functional groups of activated carbon by modification method. Surf Interfaces. 2021;22:100873. https://doi.org/10.1016/j.surfin.2020.100873.
15. Aigbe UO, Osibote OA. A review of hexavalent chromium removal from aqueous solutions by sorption technique using nanomaterials. J Environ Chem Eng. 2020;8(6):104503. https://doi.org/10.1016/j.jece.2020.104503.
16. Anyika C, Asri NAM, Majid ZA, Yahya A, Jaafar J. Synthesis and characterization of magnetic activated carbon developed from palm kernel shells. Nanotechnol Environ Eng. 2017;2(1):16. https://doi.org/10.1007/s41204-017-0027-6.
17. Arnelli, Wahyuningrum VN, Fauziah F, Astuti Y. Synthesis of surfactant modified activated carbon (SMAC) from rice husks as Ni(II) and Cr(VI) adsorbent. In: IOP Conference Series: Materials and Science Engineering, Volume 509, 13th Joint Conference on Chemistry (13th JCC), Semarang, Indonesia, 7–8 September 2018. Bristol: IOP Publishing, 2019. Article 012023. https://doi.org/10.1088/1757-899X/509/1/012023.
18. Egbosiuba TC, Abdulkareem AS, Kovo AS, Afolabi EA, Tijani JO, Bankole MT, Bo S, Roos WD. Adsorption of Cr(VI), Ni(II), Fe(II) and Cd(II) ions by KIAgNPs decorated MWCNTs in a batch and fixed bed process. Sci Rep. 2021;11(1):75. https://doi.org/10.1038/s41598-020-79857-z.
19. Padmavathy KS, Madhu G, Haseena PV. A study on Effects of pH, Adsorbent Dosage, Time, Initial Concentration and Adsorption Isotherm Study for the Removal of Hexavalent Chromium (Cr (VI)) from Wastewater by Magnetite Nanoparticles. Procedia Technol. 2016;24:585–594. https://doi.org/10.1016/j.protcy.2016.05.127.
20. Amuanyena MON, Kandawa-Schulz M, Kwaambwa HM. Magnetic Iron Oxide Nanoparticles Modified with Moringa Seed Proteins for Recovery of Precious Metal Ions. J Biomater Nanobiotechnol. 2019;10(2):142–158. https://doi.org/10.4236/jbnb.2019.102008.
21. Maikokera R, Kwaambwa HM. Interfacial properties and fluorescence of a coagulating protein extracted from Moringa oleifera seeds and its interaction with sodium dodecyl sulphate. Colloids Surf B Biointerfaces. 2007;55(2):173–178. https://doi.org/10.1016/j.colsurfb.2006.11.029.
22. Biata NR, Jakavula S, Mashile GP, Nqombolo A, Moutloali RM, Nomngongo PN. Recovery of gold(III) and iridium(IV) using magnetic layered double hydroxide (Fe3O4/Mg-Al-LDH) nanocomposite: equilibrium studies and application to real samples. Hydrometallurgy. 2020;197:105447. https://doi.org/10.1016/j.hydromet.2020.105447.
23. Mourdikoudis S, Pallares RM, Thanh NTK. Characterization techniques for nanoparticles: comparison and complementarity upon studying nanoparticle properties. Nanoscale. 2018;10(27):12871–12934. https://doi.org/10.1039/C8NR02278J.
24. Bagherzadeh M, Aslibeiki B, Arsalani N. Preparation of Fe3O4/vine shoots derived activated carbon nanocomposite for improved removal of Cr(VI) from aqueous solutions. Sci Rep. 2023;13(1):3960. https://doi.org/10.1038/s41598-023-31015-x.
25. Bediako JK, Kudoahor E, Lim CR, Affrifah NS, Kim S, Song MH, Repo E. Exploring the insights and benefits of biomass-derived sulfuric acid activated carbon for selective recovery of gold from simulated waste streams. Waste Manag. 2024;177:135–145. https://doi.org/10.1016/j.wasman.2024.02.002.
26. Kang Z, Jia X, Ma X, Wen D. Modelling and Prediction of Fe/MWCNT Nanocomposites for Hexavalent Chromium Reduction. Processes (Basel). 2023;11(12):3271. https://doi.org/10.3390/pr11123271.
27. Mittal R, Sharma A, Bhardwaj AK, Bhateria R, Bansal S, Kashyap R, Bhukal S. Removal of chromium (VI) using spirulina assisted synthesized mesoporous iron oxide nanoparticles. Inorg Chem Commun. 2023;154:110881. https://doi.org/10.1016/j.inoche.2023.110881.
28. Kumar A, Dixit CK. Methods for characterization of nanoparticles. In: Nimesh S, Chandra R, Gupta N (editors), Advances in Nanomedicine for the Delivery of Therapeutic Nucleic Acids. Duxford: Woodhead Publishing; 2017. pp. 43–58. https://doi.org/10.1016/B978-0-08-100557-6.00003-1.
29. Shekede T, Mishra AK. Moringa oleifera Seeds Extracts / Magnetite based Bionanocomposites for Hexavalent chromium Uptake. SETWM. 2019;19:55–62. https://doi.org/10.17758/EARES8.EAP1119247.
30. Zhu Q, Zhu J, Huang K. Selectivity of modified pomegranate peel for gold, platinum, and palladium: adsorption behavior, mechanism, and recovery. J Environ Chem Eng. 2024;12(2):111902. https://doi.org/10.1016/j.jece.2024.111902.
31. Ihsanullah, Al-Khaldi FA, Abu-Sharkh B, Abulkibash AM, Qureshi MI, Laoui T, et al. Effect of acid modification on adsorption of hexavalent chromium (Cr(VI)) from aqueous solution by activated carbon and carbon nanotubes. Desalin Water Treat. 2016;57(16):7232–7244. https://doi.org/10.1080/19443994.2015.1021847.
32. Boddolla S, Thodeti S. A Review On Characterization Techniques Of Nanomaterials. Int. J. Eng. Sci. Math. 2018;7(1):169–175.
33. Mihăilescu M, Negrea A, Ciopec M, Davidescu CM, Negrea P, Duțeanu N, Rusu G. Gold (III) adsorption from dilute waste solutions onto Amberlite XAD7 resin modified with L-glutamic acid. Sci Rep. 2019;9(1):8757. https://doi.org/10.1038/s41598-019-45249-1.
34. Iqbal A, Jan MR, Shah J, Rashid B. Dispersive solid phase extraction of precious metal ions from electronic wastes using magnetic multiwalled carbon nanotubes composite. Miner Eng. 2020;154:106414. https://doi.org/10.1016/j.mineng.2020.106414.
35. Mohamed Khalith SB, Rishabb Anirud R, Ramalingam R, Karuppannan SK, Dowlath MJH, Pandion K, Ravindran B, WoongChang S, Ovi D, Arasu MV, et al. WoongChang S, Ovi D, Arasu MV, Ignacimuthu S, Al-Dhabi AN, Chandrasekaran M, Arunachalam KD. Synthesis and characterization of magnetite carbon nanocomposite from agro waste as chromium

adsorbent for effluent treatment. Environ Res. 2021;202:111669. https://doi.org/10.1016/j.envres.2021.111669.

36. Timbo CC, Kandawa-Schulz M, Amuanyena M, Kwaambwa HM. Adsorptive Removal from Aqueous Solution of Cr(VI) by Green Moringa Tea Leaves Biomass. J Encap Adsorpt Sci. 2017;7(2):108–119. https://doi.org/10.4236/jeas.2017.72008.
37. Grad O, Ciopec M, Negrea A, Duțeanu N, Vlase G, Negrea P, Dumitrescu C, Vlase T, Voda R. Precious metals recovery from aqueous solutions using a new adsorbent material. Sci Rep. 2021;11(1):2016. https://doi.org/10.1038/s41598-021-81680-z.
38. El-Baz AA, Hendy I, Dohdoh AM, Srour MI. Adsorption of High Chromium Concentrations from Industrial Wastewater Using Different Agricultural Residuals. J Environ Treat Tech. 2020;9(1):122–138. https://doi.org/10.47277/JETT/9(1)138.
39. Ume OL, Ekeoma BC, Yusuf M, Al-Kahtani AA, Ubaidullah M, Sillanpää M. Batch studies of hexavalent chromium biosorption from mining wastewater using Aspergillus niger. Results Chem. 2022;4:100490. https://doi.org/10.1016/j.rechem.2022.100490.
40. Wang J, Guo X. Adsorption kinetics and isotherm models of heavy metals by various adsorbents: an overview. Crit Rev Environ Sci Technol. 2023;53(21):1837–1865. https://doi.org/10.1080/10643389.2023.2221157.
41. Ravi T, Sundararaman S. Adsorptive Separation of Hexavalent Chromium From its Aqueous and Real Water Mixtures Using Thermally Treated Country Eggshell Coated With Magnetite Nanoparticles. Russ J Phys Chem B Focus Phys. 2021;15(3):462–475. https://doi.org/10.1134/S1990793121030295.
42. Thilagavathy P, Santhi T. Adsorption of Cr (VI) Onto Low-Cost Adsorbent Developed from Acacia Nilotica Leaf Activated with Phosphoric Acid: Kinetic, Equilibrium Isotherm and Thermodynamic Studies. Int J Sci Res (Raipur). 2014;3(5):308–314.
43. Gheju M, Balcu I, Jurchescu P. Removal of hexavalent chromium from aqueous solutions by use of chemically modified sour cherry stones. Desalination Water Treat. 2016;57(23):10776–10789. https://doi.org/10.1080/19443994.2015.1040468.
44. Sherlala AIA, Raman AAA, Bello MM, Asghar A. A review of the applications of organo-functionalized magnetic graphene oxide nanocomposites for heavy metal adsorption. Chemosphere. 2018;193:1004–1017. https://doi.org/10.1016/j.chemosphere.2017.11.093.
45. Kadhom M, Abdullah G, Abdullah GH, Kadhom MA. Studying of two choline chloride's deep eutectic solvents in their aqueous mixtures. Int J Engine Res. 2016;12(9):73–80.
46. Lanaridi O, Platzer S, Nischkauer W, Betanzos JH, Iturbe AU, Del Rio Gaztelurrutia C, Sanchez-Cupido L, Siriwardana A, Schnurch M, Limbeck A, et al. Benign recovery of platinum group metals from spent automotive catalysts using choline-based deep eutectic solvents. Green Chem Lett Rev. 2022;15(2):405–414. https://doi.org/10.1080/17518253.2022.2068973.
47. Yuan Z, Liu H, Yong WF, She Q, Esteban J. Status and advances of deep eutectic solvents for metal separation and recovery. Green Chem. 2022;24(5):1895–1929. https://doi.org/10.1039/D1GC03851F.
48. Poudel A, Adhikari S, Asfaha TY, Lawrence JG, Kandage MM, Marszewski M, Kirchhoff JR. Efficient extraction and analysis of precious metals with a conducting polymer modified magnetic sorbent material. Resour Conserv Recycling. 2023;199:107199. https://doi.org/10.1016/j.resconrec.2023.107199.
49. Hashem MA, Elnagar MM, Kenawy IM, Ismail MA. Synthesis and application of hydrazono-imidazoline modified cellulose for selective separation of precious metals from geological samples. Carbohydr Polym. 2020;237:116177. https://doi.org/10.1016/j.carbpol.2020.116177.